Network Science **9** (S1): S106–S133, 2021
doi:10.1017/nws.2020.42

CAMBRIDGE UNIVERSITY PRESS

ORIGINAL ARTICLE

A simple differential geometry for complex networks

Emil Saucan[1*], Areejit Samal[2,3] and Jürgen Jost[3,4]

[1]Department of Applied Mathematics, ORT Braude College, Karmiel 2161002, Israel, [2]The Institute of Mathematical Sciences (IMSc), Homi Bhabha National Institute (HBNI), Chennai 600113, India, [3]Max Planck Institute for Mathematics in the Sciences, Leipzig 04103, Germany (email: asamal@imsc.res.in) and [4]The Santa Fe Institute, Santa Fe, New Mexico 87501, USA (email: jost@mis.mpg.de)
*Corresponding author. Email: semil@braude.ac.il

Action Editor: Hocine Cherifi

Abstract

We introduce new definitions of sectional, Ricci, and scalar curvatures for networks and their higher dimensional counterparts, derived from two classical notions of curvature for curves in general metric spaces, namely, the Menger curvature and the Haantjes curvature. These curvatures are applicable to unweighted or weighted and undirected or directed networks and are more intuitive and easier to compute than other network curvatures. In particular, the proposed curvatures based on the interpretation of Haantjes definition as geodesic curvature allow us to give a network analogue of the classical local Gauss–Bonnet theorem. Furthermore, we propose even simpler and more intuitive proxies for the Haantjes curvature that allow for even faster and easier computations in large-scale networks. In addition, we also investigate the embedding properties of the proposed Ricci curvatures. Lastly, we also investigate the behavior, both on model and real-world networks, of the curvatures introduced herein with more established notions of Ricci curvature and other widely used network measures.

Keywords: network curvature; Menger curvature; Haantjes curvature; Ricci curvature; local Gauss–Bonnet theorem; geometric embedding

1. Introduction

Till recently, mathematical analysis of complex networks was largely based upon combinatorial invariants and models (Watts & Strogatz, 1998; Barabási & Albert, 1999; Albert & Barabási, 2002; Newman, 2010; Dorogovtsev & Mendes, 2013) at the detriment of the geometric approach. Especially, theoretical developments in discrete differential geometry leading to notions of curvature (Ollivier, 2009; Forman, 2003) for graphs or networks remained largely unexplored until recently in network science (Ni et al., 2015; Sandhu et al., 2015; Sreejith et al., 2016). Noteworthy, one of the widely used combinatorial measure, the *clustering coefficient* (Watts & Strogatz, 1998), to characterize complex networks is in fact a discretization of the classical Gauss curvature (Eckmann & Moses, 2002). Lately, notions of network curvature have proven to be an important tool in the analysis of complex networks (Ni et al., 2015; Sandhu et al., 2015; Sreejith et al., 2016; Samal et al., 2018). In particular, Ollivier–Ricci curvature (Ollivier, 2009) has been extensively used in the analysis of complex networks in its various avatars (Ni et al., 2015; Sandhu et al., 2015; Asoodeh et al., 2018; Ni et al., 2019; Farooq et al., 2019). Based on Forman's work (Forman, 2003), another approach toward the introduction of Ricci curvature in the study of networks was also proposed (Sreejith et al., 2016; Weber et al., 2017). Moreover, the two above-mentioned notions of Ricci curvature in several model and real-world networks were compared (Samal et al., 2018).

© The Author(s), 2020. Published by Cambridge University Press.

https://doi.org/10.1017/nws.2020.42 Published online by Cambridge University Press

However, these two notions of Ricci curvature for networks have certain drawbacks. Their common denominator is the theoretical advanced apparatus which stands at the base of both notions of discrete Ricci curvature for networks. While Ollivier–Ricci curvature is prohibitively hard to compute in large networks, Forman–Ricci curvature is extremely simple to compute in large networks (Samal et al., 2018). On the other hand, Forman–Ricci curvature is less intuitive than Ollivier–Ricci curvature, as it is based on a discretization of the so called *Bochner-Weitzenböck formula* (Jost, 2017). These issues may deter the interdisciplinary community of engineers, social scientists, and biologists active in network science from employing these two notions of discrete Ricci curvature in their research.

Therefore, it is worthwhile to ask whether it is possible to define more intuitive notions of curvature (specifically, Ricci curvature) for networks which are modeled using the simple framework of graphs. The answer to this quandary is immediate after the realization that the simplest, more general, geometric notion at our disposal is that of metric space. Furthermore, unweighted and weighted graphs can be easily endowed with a metric, be it the combinatorial weights, the path distance, the given weights, the Wasserstein metric (also called the Earth mover's distance) (Vaserstein, 1969), or a metric such as the path degree metric (Dodziuk & Kendall, 1986; Keller, 2015) that can be easily obtained from the given weights. For metric spaces, there indeed exist a number of simple and intuitive notions of curvature, and in particular, two definitions of curvature of curves which go back to Menger (1930) and Haantjes (1947), respectively. By partially extending ideas previously applied in the context of imaging and graphics (*PL* manifolds in general) (Saucan, 2015; Gu & Saucan, 2013; Saucan & Weber, 2018), we show that the definitions of Menger (1930) and Haantjes (1947) allow us to naturally define Ricci and scalar curvatures for networks and hypernetworks including unweighted, weighted, undirected, and directed ones.

The simplest and better known among the two notions of metric curvature is the Menger curvature. Notably, the Menger curvature defined for metric triangles naturally allows us to define scalar and Ricci curvatures for networks, hypernetworks, simplicial complexes, and clique complexes including unweighted, weighted, undirected, and directed ones. Furthermore, we show that this approach holds not only for the usual Euclidean model geometry but also for hyperbolic and spherical background geometry. We believe this is an important feature of the Menger curvature due to the following reason. Currently, while network embedding is commonly considered, such embedding is either purely combinatorial or, at most, equipped with an undescriptive Euclidean geometry which is decoupled from the one of the ambient space, and thus, a vital part of the expressiveness of the embedding is lost.

In comparison to the Menger curvature, Haantjes curvature is far less familiar among researchers but is a much more flexible notion. This is because Haantjes curvature is not restricted solely to triangles, but rather holds for general metric arcs. In consequence, Haantjes curvature presents two distinct advantages. First, it is applicable to any 2-cell, not just to triangles. Second, it can be better used as discrete version of the classical geodesic curvature (of curves on smooth surfaces). In consequence, Haantjes curvature has a clear advantage over Menger curvature as it is applicable to networks or graphs, without *any assumption on the background geometry*. In fact, not only can it be employed in networks of *variable curvature* but it can also be used to *define* the curvature of such a discrete space. In effect, this allows us to study the *intrinsic*, not just the *extrinsic*, geometry of networks. From a practical view of applications, the definition of Haantjes curvature allows inference of geometric, highly descriptive properties from its given characteristic, rather than presume them. From a more theoretical perspective but still with practical importance, for instance, while predicting the long time behavior, Haantjes curvature enables us to study networks as geometric spaces in their own right, not just as graphs realized in some largely arbitrary ambient familiar space.

We should emphasize that there is not a single, restricted motivation residing behind our quest for a purely metric differential geometry for networks. To be sure, the search for faster and more

https://doi.org/10.1017/nws.2020.42 Published online by Cambridge University Press

efficient computational tools is one of the reasons we adopted this path, but it is not the only one, nor is it, by far, the most important one.

A substantial motivation behind the choice of the metric route toward the geometrization of networks stems from the fact that it allows us to consistently define and study the *intrinsic* geometry of networks, as opposed to the more common approach via *extrinsic* geometry, that is by embedding the networks in suitable ambient space, and studying the geometric properties induced by the surrounding space. Lately, this embedding space has usually been taken to be the hyperbolic plane or space, given the understanding that, in a sense, it combines the efficiency and convenient visualization, mostly using the Poincaré models, see, e.g. Boguná (2010; 2020).

While the later approach is more innate and conducive to intuitive illustrations, such embeddings are, apart from the very stringent *isometric embeddings*, distorting. In contrast, the intrinsic approach, that is the study of networks *per se*, is independent of any specific embedding, hence of the necessary additional computations and also of any distortion. Moreover, this approach allows for the independent study of such powerful tools as the Ricci flow, without the vagaries associated to the embedding in an ambient space of certain dimension (see, e.g. Saucan (2012a) and the bibliography therein). Indeed, the development of a purely metric, intrinsic geometry of networks is the driving motivation of Sections 3.1 and 4.

Our approach to the development of a metric, intrinsic geometry for networks follows the Riemannian paradigm to geometry, more specifically its *PL* (and polyhedral) avatar. In particular, we follow the classical approach to *PL* geometry (and topology), in particular the pioneering works of Stone (1973; 1976) on the discretization of sectional and Ricci curvatures. See also Gu & Saucan (2013) for a more recent metric extension of Stone's ideas. In this approach, polygons (i.e. the two-dimensional elements in a polyhedral manifold) incident to an edge are the direct and natural *PL* analogue of the 2-sections. Therefore, by defining their curvature, one defines the curvature of the *PL* (polyhedral) 2-sections. Haantjes curvature (and, by passing to the dual complex whenever possible, Menger curvature as well) allows for what represents, we believe, a definition of sectional curvature having clear geometric content. This route not only allows an integrated and simple approach to the geometrization of networks, it is also, in a sense, the most natural and direct approach to this problem, given that *PL* manifolds represent the geometric class closest to graphs or networks, on which proper and consistent differential geometry has been developed. Moreover, given the recent growing interest of the network community in the study of multiplex- and hypernetworks (as well as other higher dimensional generalizations of networks), viewing networks as *PL* (and more general polyhedral manifolds) allows one not only to ration by analogy, but in fact provides us with arguably the best modeling tool.

We would also like to add that given the lack of smoothness of the graph structure, hence of the full force of the differential geometric apparatus, each discretization of curvature captures, in the network context, only an essential aspect of the classical notion, and as such, it can satisfy only a restricted set of the full gamut of properties of the classical notion. Therefore, it is not possible to find "the best" discrete curvature, but rather the best one suited for a certain task, in specific type of networks. This is exemplified in the sequel by the comparison between different notions of discrete Ricci curvature; see also the discussion on the comparative advantages of Ollivier–Ricci and Forman–Ricci curvature in Samal et al. (2018). It is, therefore, desirable to devise different notions of discrete curvature and explore their specific advantages for various task. The present paper represents, therefore, a step in this quest.

The remainder of the paper is structured as follows. In Section 2, we introduce the Menger curvature. In Section 3, we introduce Haantjes curvature, its generalizations and extensions, as well as its use in the introduction of local Gauss–Bonnet theorem for networks. In Section 4, we provide a brief overview of the embedding properties of the metric curvatures presented here. In Section 5, we present empirical results from analysis of the Menger curvature and the Haantjes curvature in various model and real-world networks. In Section 6, we conclude with a summary and future outlook. In Appendix A, we present the mutual relationship between the two metric

https://doi.org/10.1017/nws.2020.42 Published online by Cambridge University Press

curvatures, the Menger curvature and the Haantjes curvature, and also their connections to the classical notion of curvature for curves. Some of the results reported in this manuscript were recently presented in a conference proceeding (Saucan et al., 2019b).

2. Menger curvature

The simplest, most elementary manner, of introducing curvature in metric spaces is due to Menger (1930). Here, one simply defines the curvature $K(T)$ of a triangle T, i.e., a metric triple of points with sides of lengths a, b, c as $\frac{1}{R(T)}$, where $R(T)$ is the radius of the circle circumscribed to the triangle. An elementary computation yields

$$\kappa_{M,E}(T) = \frac{1}{R(T)} = \frac{abc}{4\sqrt{p(p-a)(p-b)(p-c)}}, \tag{1}$$

where $p = \frac{(a+b+c)}{2}$ denotes the half-perimeter of T.

Remark. The notion of curvature introduced above might appear somewhat counterintuitive, given that it prescribes to a triangle the curvature of its circumscribed circle. Thus, triangles of various shapes may have the same Menger curvature. Note that what appears as a more intuition of curvature, namely the so called *aspect ratio* is introduced in Section 3.3. While this notion is widely employed as such in graphics (and, under other names, in geometry and geometric analysis), it does not, however, represent a proper curvature notion (see Section 3.3).

However, there is conceptual problem with the above definition which utilizes the geometry of the Euclidean plane. In the general setting of networks, it is not natural to assume a Euclidean background. This is analogous to the geometry of surfaces, where the metric need not be Euclidean, but could be spherical, hyperbolic, or of varying Gauss curvature. For example, embedding networks in hyperbolic plane and space is becoming quite common (Bianconi & Rahmede, 2017; Krioukov et al., 2010; Zeng et al., 2010).

Of course, one may formulate a spherical or hyperbolic analogue of Equation (1), see, e.g. Janson (2015). The spherical version is

$$\kappa_{M,S}(T) = \frac{1}{\tan R(T)} = \frac{\sqrt{\sin p \sin(p-a) \sin(p-b) \sin(p-c)}}{2 \sin\frac{a}{2} \sin\frac{b}{2} \sin\frac{c}{2}}, \tag{2}$$

whereas the hyperbolic version is

$$\kappa_{M,H}(T) = \frac{1}{\tanh R(T)} = \frac{\sqrt{\sinh p \sinh(p-a) \sinh(p-b) \sinh(p-c)}}{2 \sinh\frac{a}{2} \sinh\frac{b}{2} \sinh\frac{c}{2}}. \tag{3}$$

Note that, in the setting of networks, the constant factors "4" and "2," respectively, appearing in the denominators of the above equations are less relevant, and they can be discarded in this context.

Remark. The factors $(p-a), (p-b), (p-c)$ in the definition above are, in fact, the so called *Gromov products* of the vertices of T, which are employed in the definition of *Gromov δ-hyperbolicity* (Gromov, 2007). Thus, Menger curvature (and a related, simpler metric invariant that we introduce in Section 3.3) may be viewed as a local version of the Gromov hyperbolicity. Given the fact that Gromov hyperbolicity is a global property, hence difficult to compute, it is good to be able to substitute, whenever possible, a local related notion of curvature. Moreover, while Gromov hyperbolicity represents a coarse, global notion of sectional curvature, the Menger curvature which we propose herein is a local, notion of sectional curvature, thus fitting better the classical Riemannian paradigm of the development of curvature, first locally, then globally,

https://doi.org/10.1017/nws.2020.42 Published online by Cambridge University Press

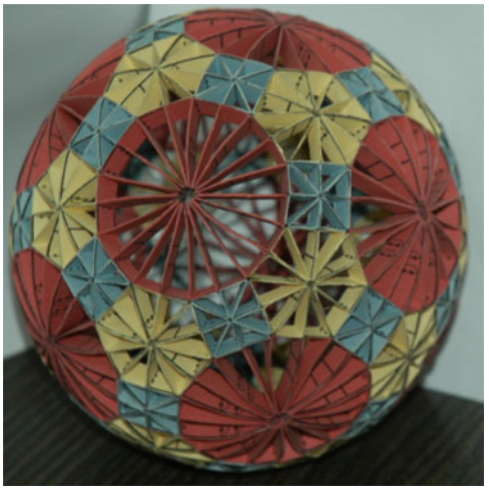


Figure 1. The spherical network representing the 1-skeleton of the canonical triangulation with fundamental triangles of the spherical counterpart of the *truncated icosidodecahedron* (see also Figure 3).

that we adopted herein. This is especially meaningful if "local-to-global" properties, which play an important role in metric geometry (Burago et al., 2001; Perelman, 1991; Plaut, 2002), can be proven for Haantjes curvature.

Examples of computing Menger curvature with spherical background geometry

(1) Let $\triangle ABC$ be a spherical triangle with angles $\alpha = \beta = \gamma = \frac{\pi}{2}$ on a sphere of radius 1. Then the length of the sides of the triangle, $a = b = c = \frac{\pi}{2}$, and the formula above renders $\kappa_{M,S}(\triangle ABC) = \frac{\sqrt{2}}{2}$.
(2) The 1-skeleton of the triangulation of the sphere consisting of the fundamental triangles of a spherical counterpart of an Archimedean polyhedron (see Figure 1) represents a spherical network. The side of the spherical faces is taken to be two units. The fundamental triangle of an n-gonal face has angles $(\frac{\pi}{2}, \frac{\pi}{3}, \frac{\pi}{n})$, $n = 4, 6, 10$. Hence, the remaining sides of the triangles, thence their Menger curvatures, can be computed using the classical formulas of spherical trigonometry, see, e.g. Janson (2015).

Examples of computing Menger curvature with hyperbolic background geometry

(1) The hyperbolic plane admits a tessellation with triangles of angles $(\frac{\pi}{2}, \frac{\pi}{3}, \frac{\pi}{7})$. The dual graph represents also a tessellation with regular (hyperbolic) squares, hexagons, and 14-gones, symbolically denoted as $(4, 6, 14)$. It can be viewed as the *Cayley graph* of the group of the symmetries of the tessellation above, as generated by the reflections in the sides of the triangles, see, e.g. Epstein et al. (1992). Assuming that the edge is opposite to the angle of measure $\frac{\pi}{7}$, one can compute the remaining sides using the classical formulas of hyperbolic trigonometry, see, e.g. Janson (2015).
(2) It is possible to tessellate the hyperbolic space with regular dodecahedra having all the faces with angles equal to $\frac{\pi}{2}$, see, e.g. Thurston (1997). Then the fundamental triangle of the faces of these dodecahedra has angles $(\frac{\pi}{5}, \frac{\pi}{4}, \frac{\pi}{2})$. Normalizing the sides of the dodecahedra, such that half of its length be equal to 1, the *hyperbolic law of sinuses*, see, e.g. Janson (2015), gives $\sinh a = \frac{2\sqrt{2}}{2} \cdot \frac{\sinh 1}{\sinh \pi/5}$ for the side opposite the angle of measure $\frac{\pi}{4}$, and $\sinh a = \frac{\sinh 1}{\sinh \pi/5}$ for the side opposite the right angle. From these, the $\kappa_{M,H}(T)$ of the triangle can be readily computed.

https://doi.org/10.1017/nws.2020.42 Published online by Cambridge University Press

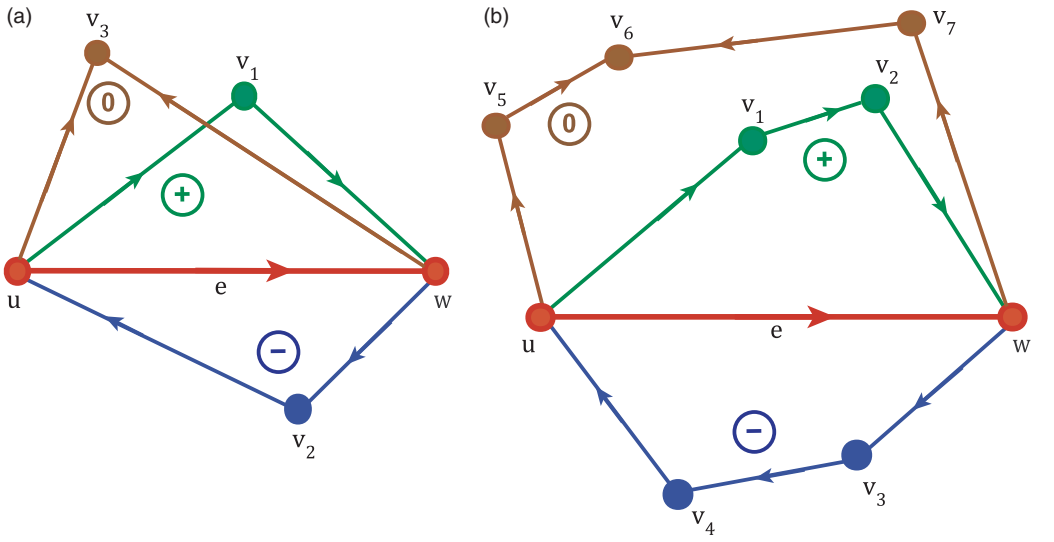


Figure 2. Sign convention for (a) directed triangles and (b) directed polygons. This specific choice of the direction of triangles (while not the only possible one) is by now commonly accepted by many in the complex networks community (see, e.g. Saucan et al. (2019b)), and it is motivated largely by the work of Alon and colleagues on network motifs (Milo et al., 2002). More precisely, positively oriented triangles correspond to feed forward loops, negatively oriented ones to feed backward loops, while zero curvature (no contribution) is attached to triangles that belong to neither of these types.

Hyperbolic geometry is considered better suited to represent the background network geometry as it captures the qualitative aspects of networks of exponential growth such as the World Wide Web, and thus, it is used as the setting for a variety of purposes. However, spherical geometry is usually not considered as a model geometry for networks because that geometry has finite diameter, hence finite growth. However, spherical networks naturally arise in at least two instances. The first one is that of global communication, where the vertices represent relay stations, satellites, sensors, or antennas that are distributed over the geo-sphere or over a thin spherical shell that can, and usually is, modeled as a sphere. The second one is that of brain networks, where the cortex neurons are envisioned, due to the spherical topology of the brain, as being distributed on a sphere or, in some cases, again on a very thin (only a few neurons deep) spherical shell, that can also be viewed as essentially spherical. One can also devise an analogous, although less explicit formula in spaces of variable curvature, but in network analysis, it is not clear where that background curvature should come from. After all, the purpose here is to define curvature, and not take it as given.

As defined, the Menger curvature is always positive. This may not be desirable, as in geometry, the distinction between positive and negative curvature is important. For directed networks, however, a sign $\varepsilon(T) \in \{-1, 0, +1\}$ is naturally attached to a directed triangle T (Figure 2), and the Menger curvature of the directed triangle is then defined, in a straightforward manner as

$$\kappa_{M,O}(T) = \varepsilon(T) \cdot \kappa_M(T)\,, \tag{4}$$

where κ_M could be the Euclidean, the spherical or the hyperbolic version, accordingly to the given setting. Note that, since in simplicial complexes, triangles adjacent to an edge represent discrete (*PL*) analogues of two-dimensional sections, the Menger curvature of each such triangle T can be naturally interpreted as the sectional curvature of T.

We can then define the Menger–Ricci curvature of an edge by averaging as in differential or piecewise linear geometry as

$$\kappa_{M,O}(e) = \mathrm{Ric}_{M,O}(e) = \sum_{T_e \sim e} \kappa_{M,O}(T_e)\,, \tag{5}$$

https://doi.org/10.1017/nws.2020.42 Published online by Cambridge University Press

where $T_e \sim e$ denote the triangles adjacent to the edge e, and the Menger-scalar curvature of a vertex is given by

$$\kappa_{M,O}(v) = \mathrm{scal}_{M,O}(v) = \sum_{e_k \sim v} \mathrm{Ric}_{M,O}(e_k) = \sum_{T \sim v} \kappa_{M,O}(T)\,, \tag{6}$$

where $e_k \sim v$ and $T \sim v$ stand for all the edges e_k adjacent to the vertex v and all the triangles T having v as a vertex, respectively. Of course, for undirected networks, the sign of $\varepsilon(T)$ is assumed to be always equal to 1.

Remark. $\mathrm{Ric}_M(e)$ captures, in keeping with the intuition behind $\kappa_M(T)$, the geodesic dispersion rate aspect of Ricci curvature. See Samal et al. (2018) for a succinct overview of the different aspects of Ricci curvature.

As indicated above, we see two drawbacks for Menger curvature as a tool in network analysis. It depends on a background geometry model, and it naturally applies only to triangles, but not to more general 2-cells. Therefore, we turn, in the next section, to Haantjes curvature, which we find more flexible in applications. (See, however, the remark below.)

Remark. It is possible to prescribe a Menger curvature for general paths as well, in the following manner. Let $\pi = v_0, v_1, \ldots, v_{n-1}, v_n$ be a path, subtended by the chord (v_0, v_n), and let $v_k, 1 \leq k \leq n-1$ be any intermediary vertex. Then v_k divides the path π into two paths $\pi_1 = v_1, \ldots, v_k$ and $\pi_2 = v_k, \ldots, v_n$. Let us denote $a = l(\pi_1), b = l(\pi_2), c = l(v_0, v_n)$. Then one can consider the Menger curvature of the metric triangle $\triangle v_0 v_k v_n$. Note that it does not depend on the choice of the vertex v_k. Again, the Menger curvature can be computed with the Euclidean, spherical, or hyperbolic flavor, according to the preferred model geometry for the given network. As already noted above, this approach has the limitation of prescribing a predefined curvature for the network. On the other hand, this approach allows for the passing to an *Alexandrov comparison* type of *coarse geometry*, see, e.g. Burago et al. (2001).

3. Haantjes curvature

Haantjes (1947) defined metric curvature by comparing the ratio between the length of an arc of curve and that of the chord it subtends. More precisely, if c is a curve in a metric space (X, d), and p, q, r are points on c, p between q and r, the Haantjes curvature is defined as

$$\kappa_H^2(p) = 24 \lim_{q,r \to p} \frac{l(\widehat{qr}) - d(q,r)}{\big(d(q,r)\big)^3}\,, \tag{7}$$

where $l(\widehat{qr})$ denotes the length, in the intrinsic metric induced by d, of the arc $\widehat{qr}$ (see also Appendix below). In the network case, $\widehat{qr}$ is replaced by a path $\pi = v_0, v_1, \ldots, v_n$, and the subtending chord by edge $e = (v_0, v_n)$. Clearly, the limiting process has no meaning in this discrete case. Furthermore, the normalizing constant "24" which ensures that, the limit in the case of smooth planar curves will coincide with the classical notion, is superfluous in this setting. This leads to the following definition of the *Haantjes curvature of a simple path* π:

$$\kappa_H^2(\pi) = \frac{l(\pi) - l(v_0, v_n)}{l(v_0, v_n)^3}\,, \tag{8}$$

where, if the graph is a metric graph, $l(v_0, v_n) = d(v_0, v_n)$. In particular, in the case of the combinatorial metric, we obtain that, for path $\pi = v_0, v_1, \ldots, v_n$ as above, $\kappa_H(\pi) = \sqrt{n-1}$. Note that considering simple paths is not a restriction, given that a metric arc is, by definition, a simple curve. However, to capture in the discrete context the local nature of the Ricci (and scalar) curvature, we shall restrict to paths π such that $\pi^* = v_0, v_1, \ldots, v_n, v_0$ is an *elementary cycle*.

https://doi.org/10.1017/nws.2020.42 Published online by Cambridge University Press

Clearly, one can extend the above definition of Haantjes curvature to directed paths in the same manner as done for the Menger curvature in the preceding section, namely

$$\kappa_{H,O}(\pi) = \varepsilon(\pi) \cdot \kappa_H(\pi)\,, \tag{9}$$

for every directed path π, where $\varepsilon(\pi) \in \{-1, 0, +1\}$ denotes the direction of path π (see also Section 3.3 below). As in the case of Menger curvature, $\varepsilon(\pi) \equiv +1$, for undirected networks.

In a straightforward manner, we can define Haantjes–Ricci curvature and Haantjes–scalar curvature, similar to the Menger curvature, as

$$\kappa_{H,O}(e) = \mathrm{Ric}_{H,O}(e) = \sum_{\pi \sim e} \kappa_{H,O}(\pi)\,, \tag{10}$$

where $\pi \sim e$ denote the paths that connect the vertices anchoring the edge e, and

$$\kappa_{H,O}(v) = \mathrm{scal}_{H,O}(v) = \sum_{e_k \sim v} \mathrm{Ric}_{H,O}(e_k)\,, \tag{11}$$

where $e_k \sim v$ stands for all the edges e_k adjacent to the vertex v. In the following, we shall, however, significantly strengthen the somewhat simplistic definition of the Haantjes–Ricci curvature presented above.

Examples of Archimedean (semi-regular) polyhedra

(1) *The truncated dodecahedron* is a typical Archimedean convex body, hence of positive combinatorial curvature concentrated at vertices. However, the two types of edges, the pentagon–hexagon ones and the hexagon–hexagon ones, in this object have Forman–Ricci curvature $\mathrm{Ric}_F(e)$ equal to -1 and -2, respectively. In contrast, the Haantjes–Ricci curvature is, by definition, always positive: $\mathrm{Ric}_H(e) = 9$ for the pentagon–hexagon edges, and $\mathrm{Ric}_H(e) = 10$ for the hexagon–hexagon edges.

(2) *The truncated octahedron* is another Archimedean polyhedron. The positivity condition for Forman–Ricci curvature for all edges does not hold here as well: $\mathrm{Ric}_F(e) = 0$ for square–hexagon edges and $\mathrm{Ric}_F(e) = -2 < 0$ for hexagon–hexagon edges. While the Haantjes–Ricci curvature is, by definition, always positive: $\mathrm{Ric}_H(e) = 8$ for the square–hexagon edges and $\mathrm{Ric}_H(e) = 10$ for the hexagon–hexagon edges. Let us also note that the edges of this object represent the *Cayley graph* of the symmetric group $S(4)$ with respect to the set of generators $\{\tau_1, \tau_2, \tau_3\}$, where τ_1, τ_2, τ_3 are the transpositions $\tau_1 = (12)$, $\tau_2 = (23)$, $\tau_3 = (34)$ (see (Epstein et al., 1992)).

It should be noted that the computation of the Ollivier–Ricci curvature for the Archimedean polyhedra above is not always possible, as they contain faces with 6 or more edges, and the combinatorial Ollivier–Ricci curvature is not defined for such cycles (Figure 3). (See also Table 1, where the Ollivier–Ricci curvature of the hexagonal planar grid is omitted for the very same reason.) This fact demonstrates one of the important relative advantages of Haantjes–Ricci curvature, namely that it is applicable to (networks containing) cycles of any length. This feature of Haantjes–Ricci curvature is of importance not only in a geometric context, such in the examples above but also in such settings as that of social and biological networks, for instance, where the length of cycles has important modeling significance.

Examples of nonconvex uniform polyhedra.

(1) *The tetrahemihexahedron* $(4.\frac{3}{2}.4.3)$ is a simple nonorientable polyhedron, representing a (minimalistic) model of the real projective plane. As such, it's Euler characteristic is equal to 1. The Forman–Ricci curvature of each edge here is equal to 1, and thus, strictly positive, whereas the Haantjes–Ricci curvature is equal to $1 + \sqrt{2}$.

https://doi.org/10.1017/nws.2020.42 Published online by Cambridge University Press

Table 1. Comparison of undirected curvatures for a number of standard grids (tessellations) of the Euclidean plane and space

Curvature type	Triangular tessellation	Square tessellation	Hexagonal tessellation	Euclidean cubulation
$\mathrm{Ric}_H(e)$	$4\pi - 2$	$4\pi - 4$	$4\pi - 2\sqrt{2}$	$8\pi - 4\sqrt{2}$
$\mathrm{Ric}_{F,r}(e)$	-8	-2	-2	-4
$\mathrm{Ric}_F(e)$	-2	0	4	4
$\mathrm{Ric}_O(e)$	1	-1	–	$-\frac{4}{3}$



Figure 3. The truncated icosidodecahedron, another Archimedean polyhedron. This is an Euclidean counterpart of the spherical polyhedron in Figure 1. There are three types of edges in this object, and the Forman–Ricci curvature for the square–hexagon, square–decagon, and hexagon–decagon edges are equal to $\sqrt{2}+\sqrt{5}$, $\sqrt{2}+3$, and $\sqrt{5}+3$, respectively. Note that the computation of the Ollivier–Ricci curvature for this Archimedean polyhedron is not possible, due to the presence of faces with 6 or more edges, since the combinatorial Ollivier–Ricci curvature is not defined for such cycles. This fact underlines one of the important relative advantages of Haantjes–Ricci curvature, namely that it is applicable to networks containing cycles of any length.

(2) *The octahemoctahedron* $(6.\frac{3}{2}.6.3)$ is the only toroidal uniform poyhedron with Euler characteristic 0. The Forman–Ricci curvature of each triangle–hexahedron edge here is equal to -1, whereas the Haantjes–Ricci curvature is equal to 3. (Note that for this uniform polyhedron the Ollivier–Ricci curvature is, again, not defined, due to the existence faces with six edges.)

(3) *The nonconvex great rhombicuboctahedron (or quasi-rhombicuboctahedron)* $(4.\frac{3}{2}.4.4)$ is composed of 8 regular triangles and 18 squares. The triangles are *retrograde*, and thus, their Haantjes–Ricci curvature should be taken with a *negative* sign. Therefore, the Haantjes–Ricci curvature of a triangle–square edge here is $\sqrt{2}-1$, and not $\sqrt{2}+1$.

Examples of three-dimensional polyhedral complexes

(1) *The Seifert–Weber dodecahedral space* is a three manifold obtained by gluing, via $\frac{3}{10}$ of a clockwise full twist, the opposite faces of a regular dodecahedron. Each edge is incident to five dodecahedra/pentagonal faces, and hence, the Forman–Ricci curvature of such edges is -7, thus corresponding to the fact that it is possible to tile the Hyperbolic space with such dodecahedra, whereas the Haantjes–Ricci curvature is equal to $\mathrm{Ric}_H(e) = 5\sqrt{3}$.

(2) *The Poincaré dodecahedral space* is a three manifold obtained by gluing, via $\frac{1}{10}$ of a clockwise full twist, the opposite faces of a regular dodecahedron. Each edge is incident to three dodecahedra/2-faces, and hence, the Forman–Ricci curvature of such edges is equal to -1, even though the Poincaré is the classical homology 3-sphere, and thus, expected to have a positive curvature. On the other hand, the Haantjes–Ricci curvature of such edges is positive, more precisely, $\mathrm{Ric}_H(e) = 3\sqrt{3}$.

https://doi.org/10.1017/nws.2020.42 Published online by Cambridge University Press

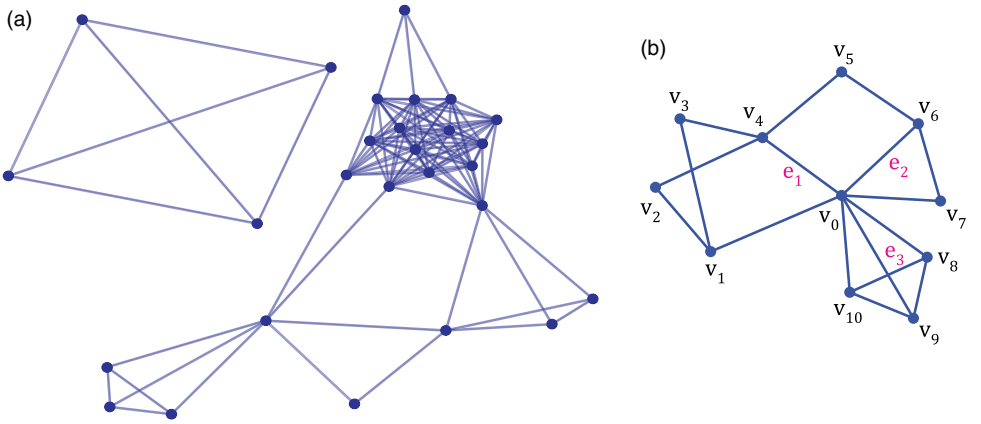


Figure 4. An example of a classic social network Zebra (Sunderasan et al., 2007) (a) Complete network. (b) A portion of the Zebra network. Note that while for the edge e_3 both Menger- and Haantjes–Ricci curvature are computable, since the 2-cycles adjacent to it are the triangles $\triangle v_0v_{10}v_9$ and $\triangle v_0v_8v_9$; for e_2 Menger–Ricci curvature can take into account only the triangle $\triangle v_0v_6v_7$, but not the quadrangle $\square v_0v_4v_5v_6$; while in the case of the edge e_1, Menger curvature would give a (false) 0 curvature, since there are no triangles, while Haantjes curvature "sees" the three adjacent quadruples, namely $\square v_0v_1v_2v_4$, $\square v_0v_1v_3v_6$, $\square v_0v_4v_5v_6$. This simple case exemplifies, therefore, the greater flexibility of Haantjes curvature, that is not restricted, as Menger's, to simplicial complexes.

Example of a classic social network. A small, classic example of a social network, Zebras (Sunderasan et al., 2007), exemplifies the fact that, given that it is defined only on triangles, Menger–Ricci curvature is not always computable, or it gives only very partial, hence distorted results (Figure 4). However, Haantjes–Ricci curvature can be easily computed for this network.

Example of a Artificial Neural Network (ANN). Figure 5 shows a small example of a weighted ANN which demonstrates the advantages of Haantjes–Ricci curvature, over Menger–Ricci, for the intelligence of networks arising in the deep learning context.

Remark. Among metric curvatures, the Haantjes curvature has several advantanges from the perspective of network science applications. Aside from the simplicity of computation in networks, Haantjes–Ricci curvature for an edge in undirected and unweighted (combinatorial) simplicial complexes can be obtained by simply counting the triangles t containing an edge e, that is

$$\mathrm{Ric}_H(e) = \sharp\{t \mid t > e\}\,. \tag{12}$$

Moreover, in k-regular undirected and unweighted simplicial complexes where each vertex is incident to precisely k edges, the (augmented) Forman–Ricci curvature of an edge e (Samal et al., 2018) is given by

$$\mathrm{Ric}_F(e) = 4 - 3\sharp\{t \mid t > e\} - 2k\,, \tag{13}$$

and thus, the formula also reduces to counting the triangles t containing an edge e. While the later formula above is also dependent on vertex degree k, for any given k the two types of Ricci curvature, Haantjes and Forman, for edges in undirected combinatorial simplicial complexes both reduce to the counting of triangles adjacent to a given edge. The computation of Haantjes–Ricci curvature above has an additional advantage of not being dependent on k. On the other hand, note that Haantjes–Ricci curvature is always positive, while Forman–Ricci curvature is mostly negative. Still, the distributions of the two curvatures, over a network, are likely to be strongly correlated. We should, however, note here that Ric_F covers further aspects of network geometry that Ric_H does not. (However, see also the discussion in the Conclusion section.)

https://doi.org/10.1017/nws.2020.42 Published online by Cambridge University Press

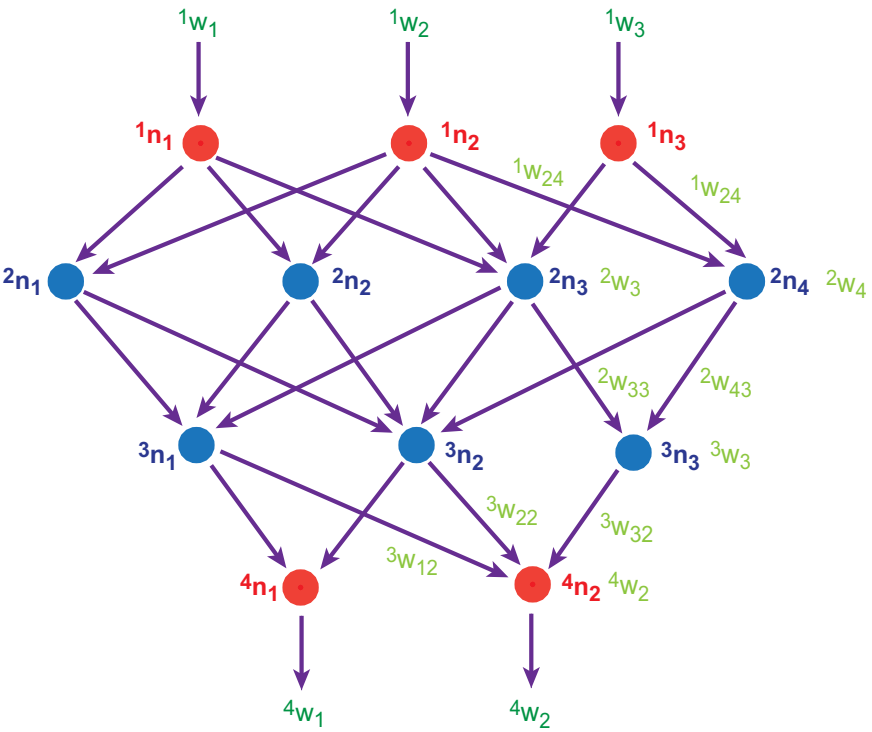


Figure 5. Schematic illustration of an artificial neural network (ANN). The nodes of the input layer, namely $^1n_1, ^1n_2, ^1n_3$ have attached weights, $^1w_1, ^1w_2, ^1w_3 \geq 0$, representing the respective inputs at these nodes. Each of the synapses $^is_{jk}$, i.e. directed edges, has a weight $^iw_{jk} \geq 0$, and these weights, together with the transfer functions ^if_k, determine the weights $^iw_{jk} \geq 0$, of the neurons ^in_k, up to and including the weights $^4w_1, ^4w_2$ of the output layer $^4n_1, ^4n_2$. Observe that there are no proper triangles, thus Forman–Ricci curvature cannot be computed for beyond separate edges and, given the essentially tree-like structure of the network, it is not very expressive; nor is the Menger–Ricci curvature definable. However, the Haantjes–Ricci curvature in any direction (of length 2) is definable. Just to exemplify, if we consider the synapses $^2s_{11}$ and $^2s_{12}$ to be endowed with combinatorial weight 1, and the weights $^3w_{12}, ^3w_{22}$ to be equal to 2 and 3, respectively, the Haantjes–Ricci curvature in the direction $^2n_1{}^3n_1{}^4n_2$ will be $13\sqrt{3}$. Needles to say, in order to truly understand the significance of this type of curvature, one need to systematically explore the various types of ANN architectures as well as the diverse transfer functions specific to each learning task, a goal that clearly goes beyond the scope of the present article.

3.1 Local Gauss–Bonnet Theorem-based sectional and Ricci curvatures

Due to its advantages over Menger curvature, we shall now use Haantjes curvature to provide stronger definitions of scalar curvature and Ricci curvature of networks. Here, the basic idea is to adapt the *local Gauss–Bonnet theorem* to this discrete setting. This approach allows us to further advance our program of providing a *PL* type geometry for networks and their higher dimensional counterparts. Recall that, in the classical context of smooth surfaces, the theorem states that

$$\int_D KdA + \sum_0^p \int_{v_i}^{v_{i+1}} k_g dl + \sum_0^p \varphi_i = 2\pi\,\chi(D)\,, \tag{14}$$

where $D \simeq \mathbb{B}^2$ is a (simple) region in the surface, having as boundary ∂D a piecewise-smooth curve π, of vertices (i.e., points where ∂D is not smooth) v_i, $i = 1, \ldots, n$, $(v_n = v_0)$, φ_i denotes the external angles of ∂D at the vertex v_i, and K and k_g denote the Gaussian and geodesic curvatures, respectively.

Let us first note that, in the absence of a background curvature, the very notion of angle is undefinable. Thus, for abstract (nonembedded) cells, there exists no *honest* notion of angle. Hence, the last term on the left side of above Equation (14) has no proper meaning, and thus, can be

https://doi.org/10.1017/nws.2020.42 Published online by Cambridge University Press

discarded. Moreover, the distances between nonadjacent vertices on the same cycle (apart from the path metric) are not defined, and thus, the second term on the left side of above Equation (14) also vanishes.

We next concentrate on the case of combinatorial (unweighted) networks. For such networks endowed with the combinatorial metric, the area of each cell is usually taken to be equal to 1. Moreover, one can naturally assume that the curvature is constant on each cell, and thus, the first term on the left side of Equation (14) reduces simply to K. In addition, given that D is a 2-cell, we have $\chi(D) = 1$. Therefore, in the absence of the definition of an angle, it is natural to define

$$K = 2\pi - \int_{\partial D} k_g dl\,. \tag{15}$$

It is tempting to next consider ∂D as being composed of segments (on which k_g vanishes), except at the vertices, thus rendering the above expression as

$$K = 2\pi - \sum_{1}^{n} \kappa_H(v_i)\,. \tag{16}$$

Remark. An alternative approach to defining the curvature of cell would be the following: Since in a Euclidean polygon, the sum of the angles equals $\pi(n-2)$, where n represents the number of vertices of the polygon, one could replace the angle sum term in Equation (14) simply by $\pi(n-2)$.

Moving to the general case of weighted networks, one cannot define a (nontrivial) Haantjes curvature for vertices, as already noted above, no proper distance between two nonadjacent vertices v_{i-1} and v_{i+1} on the same cycle can be implicitly assumed (apart from the one given by the path metric, which would produce trivial zero curvature at vertex v_i). In fact, in this general case, neither can the arc (path) $\pi = v_0, v_1, \ldots, v_n$ be truly viewed as smooth. Therefore, we have no choice but to replace the second term on the right side of above Equation (16) by $\kappa_H(\pi)$, where it should be remembered that π represents the path $v_0, v_1, \ldots, v_n$ of chord $e = (v_0, v_n)$.

We can now define the *Haantjes-sectional curvature of a 2-cell* $\mathfrak{c}$. Given an edge $e = (u, v)$ and a 2-cell $\mathfrak{c}$, $\partial\mathfrak{c} = (u = v_0, v_1, \ldots, v_n = v)$ (*relative to the edge* $e \in \partial\mathfrak{c}$), we have

$$K_{H,e}(\mathfrak{c}) = 2\pi - \kappa_{H,e}(\pi)\,, \tag{17}$$

where π denotes the path $v_0, v_1, \ldots, v_n$ subtended by the chord $e = (v_0, v_n)$ (see Figure 6), and $\kappa_{H,e}(\pi)$ denotes its respective Haantjes curvature. In the sequel, we shall refer to this version as the *strong* Haantjes–Ricci curvature of the cell $\mathfrak{c}$ to distinguish it from the simpler version each time such a differentiation is required.

Note that the definition above is much more general than the one based on Menger curvature. Indeed, not only is it applicable to cells whose boundary has (combinatorial) length greater than three, i.e., not just to triangles, it also does not presume any convexity condition for the cells, even in the case when they are realized in some model space, e.g. in $\mathbb{R}^3$. However, for simplicial complexes endowed with the combinatorial metric, the two notions coincide up to a constant. More precisely, in this case, for any triangle T, $\kappa_M(T)/\kappa_H(T) = \sqrt{3}/3$. In fact, for the case of smooth, planar curves, Menger and (unnormalized) Haantjes curvatures coincide in the limit, and furthermore, they agree with the classical concept. However, for networks there is no proper notion of convergence, a fact which allowed us to discard the factor 24 in the original definition (Equation (7)) of Haantjes curvature.

We can now define, analogous to Equation (6), the *Haantjes–Ricci curvature of an edge* e as

$$\mathrm{Ric}_H(e) = \sum_{\mathfrak{c}\sim e} K_{H,e}(\mathfrak{c}) = \sum_{\mathfrak{c}\sim e} (2\pi - \kappa_{H,e}(\pi))\,, \tag{18}$$

https://doi.org/10.1017/nws.2020.42 Published online by Cambridge University Press

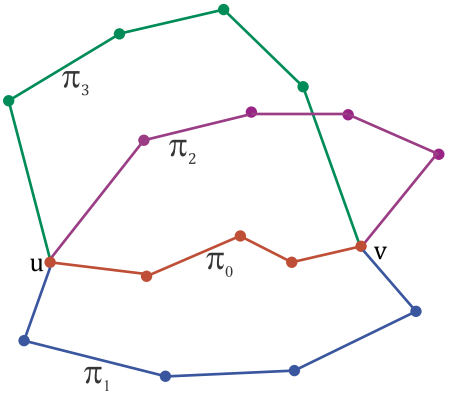


Figure 6. Haantjes–Ricci curvature in the direction $\overline{uv}$ is defined as $\mathrm{Ric}_H(\overline{uv}) = \sum_1^m K^i_{H,\overline{uv}} = \sum_1^m \kappa_{H,\overline{uv}}(\pi_i)$ where $\kappa^2_{H,\overline{uv}}(\pi_i) = \frac{l(\pi_i) - l(\pi_0)}{l(\pi_0)^3}$ $i = 1, 2, 3$; π_0 being the shortest path connecting the vertices u and v.

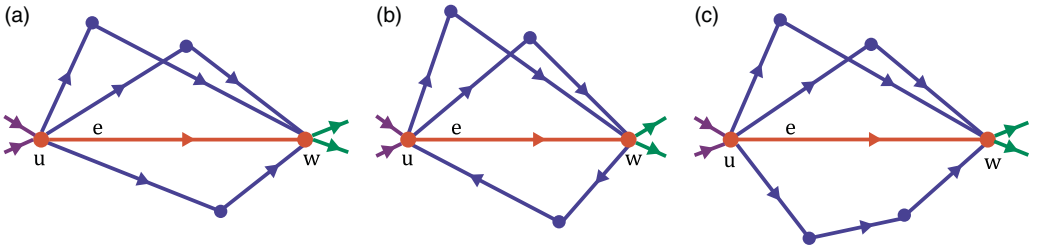


Figure 7. Haantjes–Ricci curvature $\mathrm{Ric}_{H,O}$ for directed networks, endowed with combinatorial weights: (**a**) $\mathrm{Ric}_{H,O} = 6\pi - 3$, (**b**) $\mathrm{Ric}_{H,O} = 2\pi - 1$, and (**c**) $\mathrm{Ric}_{H,O} = 6\pi - 2 - \sqrt{2}$. Note that while Forman–Ricci curvature is a counter of triangles in simplicial complexes, Haantjes–Ricci curvature represents a counter of all n-gones, since each n-gone contributes a $\sqrt{n}$ term.

where the sum is taken over all the 2-cells $\mathfrak{c}$ adjacent to e. Again, we shall call this version the *strong* Haantjes–Ricci curvature of the edge e to differentiate it from the first, simpler version, in each instance where the confusion is possible. See Figure 7 for examples of computation of Haantjes–Ricci curvature in networks, in the directed case. See Table 1[1] for the comparison on a number of (undirected) standard planar and spatial grids of the various types of Ricci curvature at our disposal.

3.2 The case of general weights

In this subsection, we return to the general case of weighted graphs. First, note that it is not reasonable to attach area 1 to every 2-cell in such graphs. However, as discussed in (Horak & Jost, 2013) and Saucan & Weber (2018), it is possible to endow cells in an abstract weighted graph with weights that are both derived from the original ones and have a geometric content. For instance, in the case of unweighted social or biological networks, endowed with the combinatorial metric, one can designate to each face, instead of the canonical combinatorial weight equal to 1, a weight that *penalizes* the faces with more edges, and thus, reflecting the weaker mutual connections between the vertices of such a face. Thus, it is possible to derive a proper local Gauss–Bonnet formula for such general networks, in a manner that still retains the given data, yet captures the geometric meaning of area, volume, etc. Thus, when considering any such geometric weight $w_g(\mathfrak{c}^2)$ of a 2-cell $\mathfrak{c}^2$, the appropriate form of the first term on the left side of Equation (14) becomes

$$Kw_g(\mathfrak{c}^2)\,, \tag{19}$$

https://doi.org/10.1017/nws.2020.42 Published online by Cambridge University Press

and the fitting form of Equation (17)

$$K_{H,e}(\mathfrak{c}) = -\frac{1}{w_g(\mathfrak{c}^2)}\left(2\pi - \kappa_{H,e}(\pi)\right) . \tag{20}$$

Before passing to the problem of extending the above definition to the case of general weights, let us note that the observations above regarding Menger curvature for directed networks apply also to Haantjes curvature, after properly extending the notion to directed 1-cycles of any length and not just to directed triangles (see Figure 2). Again, as for the Menger curvature, considering directed networks actually simplifies the problem, in the sense that it allows for variable curvature (and not just one with constant sign). For general edge weights, we have the problem that the *total weight* $w(\pi)$ of a path $\pi = v_0, v_1, \ldots, v_n$ is not necessarily smaller than the weight of its subtending chord $e = (v_0, v_n)$ [2], thus Haantjes' definition cannot be applied. However, we can turn this to our own advantage by reversing the roles of $w(\pi)$ and $w(v_0, v_n)$ in the definition of the Haantjes curvature and assigning a minus sign to the curvature of cycles for which this occurs. Thus, this approach actually allows us to define a variable sign Haantjes curvature of cycles (hence, a Ricci curvature as well), even if the given network is not a naturally directed one.

Note that the case when $w(v_0, v_1, \ldots, v_n) = w(v_0, v_n)$, i.e., that of zero curvature of the 2-cell $\mathfrak{c}$ with $\partial\mathfrak{c} = v_0, v_1, \ldots, v_n, v_0$ straightforwardly corresponds to the splitting case for the path metric induced by the weights $w(v_i, v_{i+1})$.

Indeed, the method suggested above reduces to the use of the path metric, in most of the cases. One can always pass to the path metric and apply to it the Haantjes curvature. Beyond the complications that this might induce in certain cases, it is, in our view, less general, at least from a theoretical viewpoint, since it necessitates the passage to a metric. However, in the case of most general weights, i.e. both vertex and edge weights, one has to pass to a metric. We find the *path degree metric* (see, e.g. Keller (2015)) especially alluring as it is both simple and has the capacity to capture, in the discrete context, essential geometric properties of Riemannian metrics. However, we also refer the reader to Saucan & Appleboim (2005) for an ad hoc metric devised precisely for use on graphs in tandem with Haantjes curvature.

3.3 A further generalization

Note that Equations (7) and (8) are meaningful not only for a single edge, we can consider any two vertices u, v that can be connected by a path π. Among the simple paths $\pi_1, \ldots, \pi_m$ connecting the vertices, the shortest one, i.e., the one for which $l(\pi_{i_0}) = \min\{l(\pi_1), \ldots, l(\pi_m)\}$ is attended represents the *metric segment* of ends u and v. Therefore, given any two such vertices, we can define the Haantjes–Ricci curvature in the direction $\overline{uv}$ to be

$$\mathrm{Ric}_H(\overline{uv}) = \sum_1^m K^i_{H,\overline{uv}} = \sum_1^m \kappa_{H,\overline{uv}}(\pi_i), \tag{21}$$

where $K^i_{H,\overline{uv}}$ denotes the Haantjes–Ricci curvature of the cell $\mathfrak{c}_i$, where $\partial\mathfrak{c}_i = \pi_i\pi_0^{-1}$, relative to the direction $\overline{uv}$, and where

$$\kappa^2_H(\pi_i) = \frac{l(\pi_i) - l(\pi_0)}{l(\pi_0)^3}, \tag{22}$$

and where the paths $\pi_1, \ldots, \pi_m$ satisfy the condition that $\pi_i\pi_0^{-1}$ is an *elementary cycle*. This represents a locality condition in the network setting.

Remark. Any of the paths π_i above can be viewed, according to Stone (1976) as a *variation* of the geodesic $\overline{uv}$. Thus, in the setting of metric measure spaces (Villani, 2009) and for *PL* manifolds (Stone, 1976), Equation (21) connects in the network context *Jacobi fields* to Ricci curvature as in the classical case, see, e.g. Jost (2017).

https://doi.org/10.1017/nws.2020.42 Published online by Cambridge University Press

We conclude this section by noting that both the version of the curvature for directed networks and weighted networks can be extended, *mutatis mutandis*, to this generalized definition.

Remark. For the case of networks and simplicial complexes, it is useful to note that Equation (8) for a triangle $T = T(uvw)$ reduces to

$$\kappa_H^2(T) = \frac{d(u,v) + d(v,w) - d(u,w)}{(d(u,w))^3}\,. \tag{23}$$

Thus, Haantjes curvature of triangles is closely related to two other measures, namely the *excess* $\mathrm{exc}(T)$ and *aspect ratio* $\mathrm{ar}(T)$, that are defined as follows:

$$\mathrm{exc}(T) = \max_{v\in\{u,v,w\}} \left(d(u,v) + d(v,w) - d(u,w)\right), \tag{24}$$

and

$$\mathrm{ar}(T) = \frac{exc(T)}{d(T)}\,, \tag{25}$$

where $d(T)$ denotes the diameter of a triangle $T = T(uvw)$. There are strong connections between the excess, aspect ratio, and curvature. In particular, for the normalized Haantjes curvature introduced above, we have the following relation between the three notions:

$$\kappa_H^2(T(v)) = \frac{e(T(v))}{d^3}\,, \tag{26}$$

that is

$$\kappa_H(T(v)) = \frac{\sqrt{\mathrm{ar}(T(v))}}{d}\,. \tag{27}$$

Since the factor $\frac{1}{d}$ has the role of ensuring that, in the limit, the curvature of a triangle will have the dimensionality of the curvature at a point of a planar curve, the aspect ratio can be viewed as a (skewed), unnormalized version of the curvature, and Haantjes curvature can be viewed as a *scaled* version of excess. Thus, curvature can be replaced by these surrogates, as the notion of scale is not of true import in many aspects of network characterization. Also, for the global understanding of the shape of networks, it is useful to compute, as is common in the manifold context, the *maximal* excess and *minimal* aspect ratio over all triangles in the network.

Remark. Note that Equations (23) and (24) above again contain Gromov products (Gromov, 2007) that already appeared in the definition of Menger curvature.

4. Embedding properties

As noted in the Introduction section, while studying complex networks, they are often considered for convenience to be equipped with the combinatorial metric, or they are considered to be topologically embedded in some model space and endowed with the induced (*extrinsic*) metric, e.g. the hyperbolic one. However, at least in many instances, a more realistic approach would be to consider the networks to be endowed with an *intrinsic* metric, obtained via some expressive (i.e., essential properties preserving) manner, from the weights assigned to vertices and edges in the network. In this case, a natural question to ask is whether a (topological) embedding of the network into an ambient space will preserve the metric, or in other words, whether such an embedding is an *isometric* one.

Evidently, Haantjes–Ricci curvature, due to its purely metric definition, is *geometric embedding invariant*: An isometric embedding will also preserve the curvature as is the case for Menger–Ricci

https://doi.org/10.1017/nws.2020.42 Published online by Cambridge University Press

curvature. Moreover, in the case where face weights are combinatorial, the sectional curvatures of faces, and hence, the Haantjes–Ricci curvatures are dependent solely on the metric structure of the edges, that is, Ric_H is a *strong geometric embedding invariant* therefore face areas or weights are also preserved by an isometric embedding. However, in the case where face weights are general, the Haantjes–Ricci curvature is dependent on the face weights, as a consequence of Equation (20) above, and we have the following result for general weighted networks.

Proposition 4.1. *Let* $(\mathscr{N}, \mathscr{W})$ *be a weighted network with general weights. Then, the Haantjes–Ricci curvature* Ric_H *is a geometric embedding invariant, however, not a strong geometric embedding one.*

Remark. Any topological embedding that preserves edge and 2-face cell weights is a strong geometric embedding. In particular, for combinatorial (unweighted) networks, the Haantjes–Ricci curvature Ric_H is a strong geometric embedding invariant.

5. Application to model and real-world networks

In this section, we explore the two notions of metric curvature introduced herein, in different types of model networks and real-world complex networks. Furthermore, we compare the two notions of metric curvature with existing network measures (including discrete notions of Ricci curvature) in both model and real-world complex networks.

5.1 Network datasets

For this empirical exploration, we considered three models of undirected and unweighted complex networks, four undirected and unweighted real networks, and two directed and unweighted real networks.

The three models of undirected and unweighted complex networks considered here include the Erdös–Rényi (ER) model (Erdös & Rényi, 1961), the Watts–Strogatz (WS) model (Watts & Strogatz, 1998), and the Barabási–Albert (BA) model (Barabási & Albert, 1999). The ER model generates an ensemble of random graphs $G(n, p)$ where n is the number of vertices and p is the probability that any pair of vertices are connected via an edge in the network. The WS model generates small-world graphs with high clustering and small average path length. The parameters of the WS model are the number n of vertices, the number k of nearest neighbors to which each vertex is connected in the initial network, and the rewiring probability β of edges in the initial network. The BA model generates scale-free graphs with power-law degree distribution. The parameters of the BA model are the number n of vertices in the final network, the number m_0 of vertices in the initial network, and the number m of existing vertices to which a new vertex is connected to at each step of this growing network model. Notably, the BA model uses a preferential attachment scheme whereby high-degree vertices have a higher chance of acquiring new edges than low-degree vertices at each step of this growing network model.

The 4 undirected and unweighted real-world networks considered here are as follows. The Karate club network consists of 34 vertices representing members of the club, and 78 edges representing ties between pairs of members of the club, and this dataset was collected by Zachary in (1977). The Euro road network (Šubelj & Bajec, 2011) consists of 1174 vertices representing cities in Europe and 1417 edges representing roads in the international E-road network linking different cities. The yeast protein interaction network (Jeong et al., 2001) consists of 1870 vertices representing proteins in *Saccharomyces cerevisiae* and 2277 edges representing interactions between pairs of proteins. The US Power Grid network (Leskovec et al., 2007) consists of 4941 vertices representing generators or transformers or substations in USA and 6594 edges representing power supply lines linking them. The two directed and unweighted real-world networks considered here

https://doi.org/10.1017/nws.2020.42 Published online by Cambridge University Press

are as follows. The Air traffic control network (Kunegis, 2013) consists of 1226 vertices representing airports and 2613 directed edges representing preferred routes between airports. The *E. coli* transcriptional regulatory network (TRN) (Salgado et al., 2013) consists of 3073 vertices representing genes and 7853 directed edges representing control of target gene expression through transcription factors.

5.2 Distribution of metric curvatures in networks

We have investigated the distribution of the two notions of metric curvature, namely, Menger–Ricci curvature and Haantjes–Ricci curvature in model networks considered here. Note that the Menger–Ricci curvature of edges in considered networks was computed using Equation (6) with Euclidean background geometry. In Figure 8, we display the distribution of Menger–Ricci curvature of edges in ER, WS, and BA networks with 1000 vertices and average degree 4. From the figure, it is seen that the distribution of Menger–Ricci curvature of edges is broader in BA networks in comparison to WS networks which in turn is broader in comparison to ER networks, and this trend is preserved even when one compares ER, WS, and BA networks with 1000 vertices and average degree 6 or 8 (data not shown).

Note that the Haantjes–Ricci curvature of edges in considered networks was computed using Equation (10). Due to computational constraints, we only consider simple paths π_i of length ≤ 5 between the two vertices anchoring any edge while computing its Haantjes–Ricci curvature using Equation (10). In Figure 9, we display the distribution of Haantjes–Ricci curvature of edges in ER, WS, and BA networks with 1000 vertices and average degree 4. From the figure, it is seen that the distribution of Haantjes–Ricci curvature of edges is very broad in BA networks in comparison to WS or ER networks, and this trend is preserved even when one compares ER, WS, and BA networks with 1000 vertices and average degree 6 or 8 (data not shown).

In Figure 10, we display the distribution of Haantjes–Ricci curvature of edges in four undirected and unweighted real networks considered here. In Figure 11, we display the distribution of Haantjes–Ricci curvature of directed edges in two directed and unweighted real networks considered here. As noted earlier, the Haantjes–Ricci curvature of directed edges can have negative value (unlike in the undirected and unweighted cases).

5.3 Correlation between the two metric curvatures

We next investigated the correlation between the two notions of metric curvature, namely, Menger–Ricci curvature and Haantjes–Ricci curvature in model and real networks considered here. Recall that, due to computational constraints, the computation of Haantjes–Ricci curvature of edges in considered networks using Equation (10) was restricted to simple paths π_i of maximum length ≤ 5 between the two vertices anchoring the edge under consideration. Furthermore, we have also studied the correlation between Menger–Ricci curvature and Haantjes–Ricci curvature in model and real networks as a function of the maximum length of simple paths π_i that are included in Equation (10) while computing the Haantjes–Ricci curvature.

In Table 2, we report the correlation between Menger–Ricci and Haantjes–Ricci curvature in model and real networks analyzed here. As expected, the Menger–Ricci curvature is perfectly correlated with Haantjes–Ricci curvature when the computation is restricted to paths of maximum length up to two or triangles (Table 2). However, the positive correlation between Menger–Ricci and Haantjes–Ricci curvature decreases with increase in the maximum length of paths accounted in the computation (Table 2). Specifically, Menger–Ricci and Haantjes–Ricci curvatures have minimal correlation in ER networks and moderate correlation in WS networks when paths of maximum length up to 5 are accounted in the computation. In contrast, there is high positive correlation between Menger–Ricci and Haantjes–Ricci curvatures in BA networks even when paths of maximum length up to 5 are accounted in the computation (Table 2). In real networks, we

https://doi.org/10.1017/nws.2020.42 Published online by Cambridge University Press

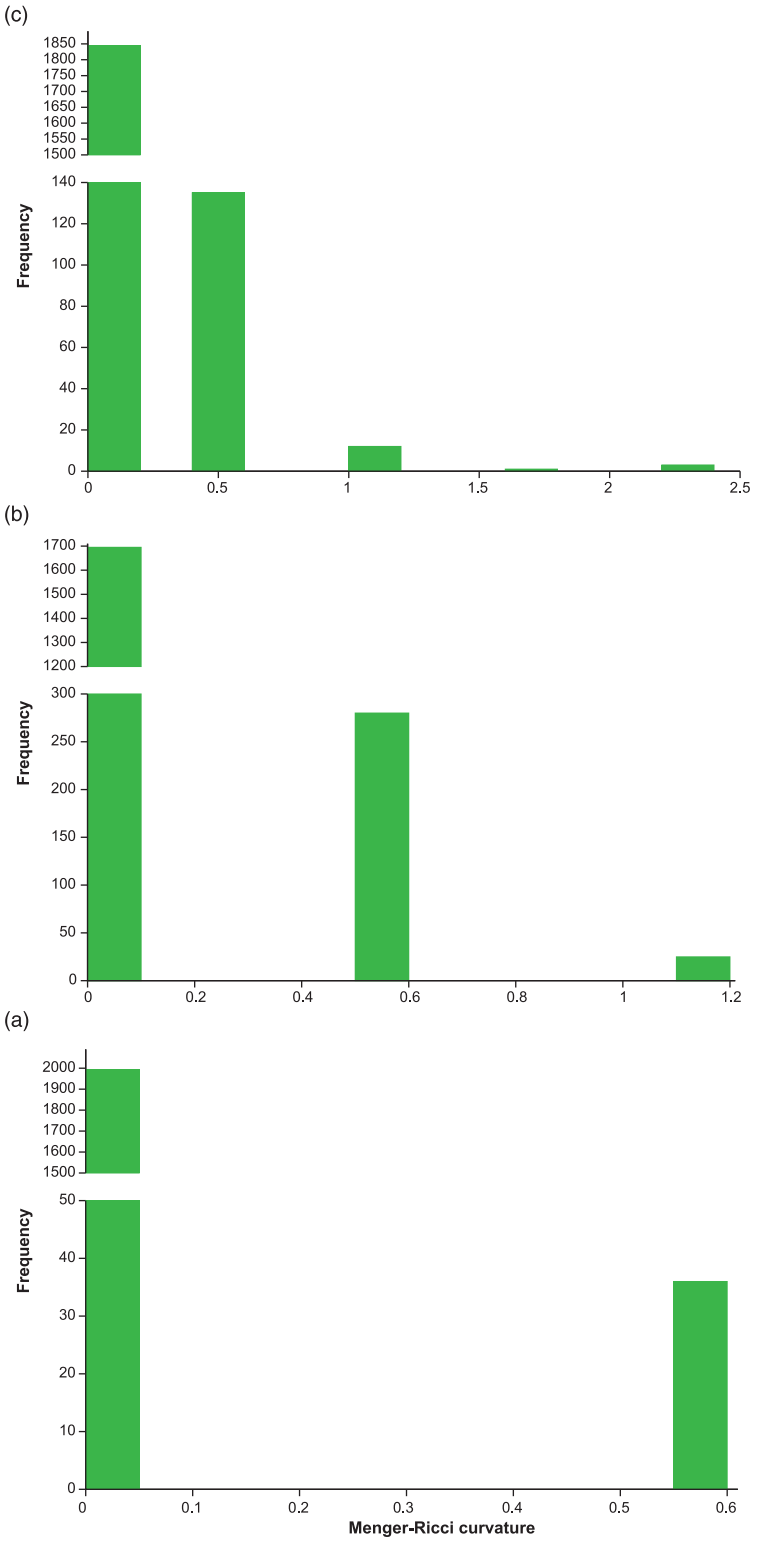


Figure 8. Distribution of Menger-Ricci curvature in model networks. **(a)** ER network, **(b)** WS network, and **(c)** BA network with 1000 vertices and average degree 4.

https://doi.org/10.1017/nws.2020.42 Published online by Cambridge University Press

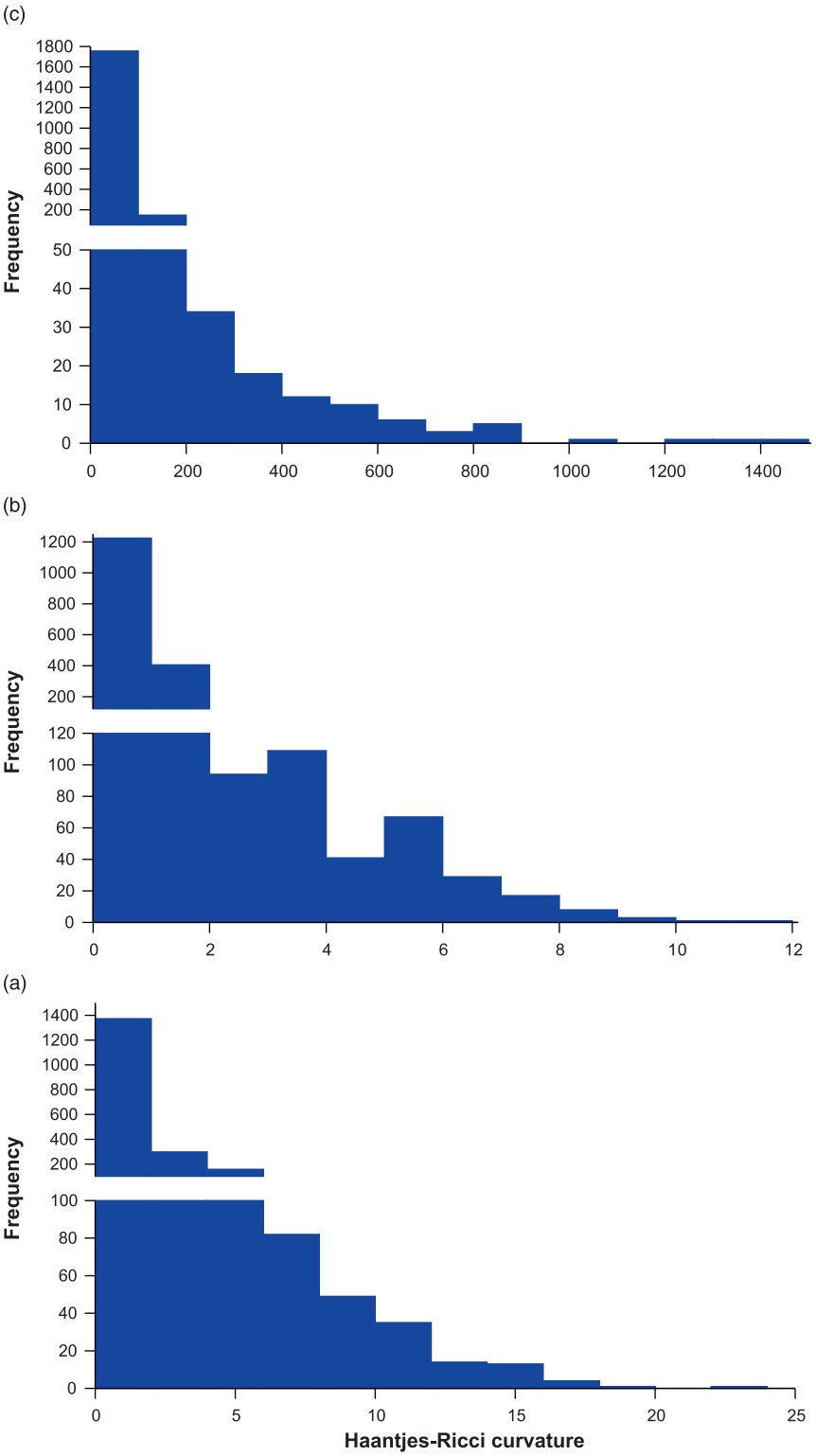


Figure 9. Distribution of Haantjes–Ricci curvature in model networks. (**a**) ER network, (**b**) WS network, and (**c**) BA network with 1000 vertices and average degree 4. Here Haantjes–Ricci curvature is given by Equation (10).

https://doi.org/10.1017/nws.2020.42 Published online by Cambridge University Press

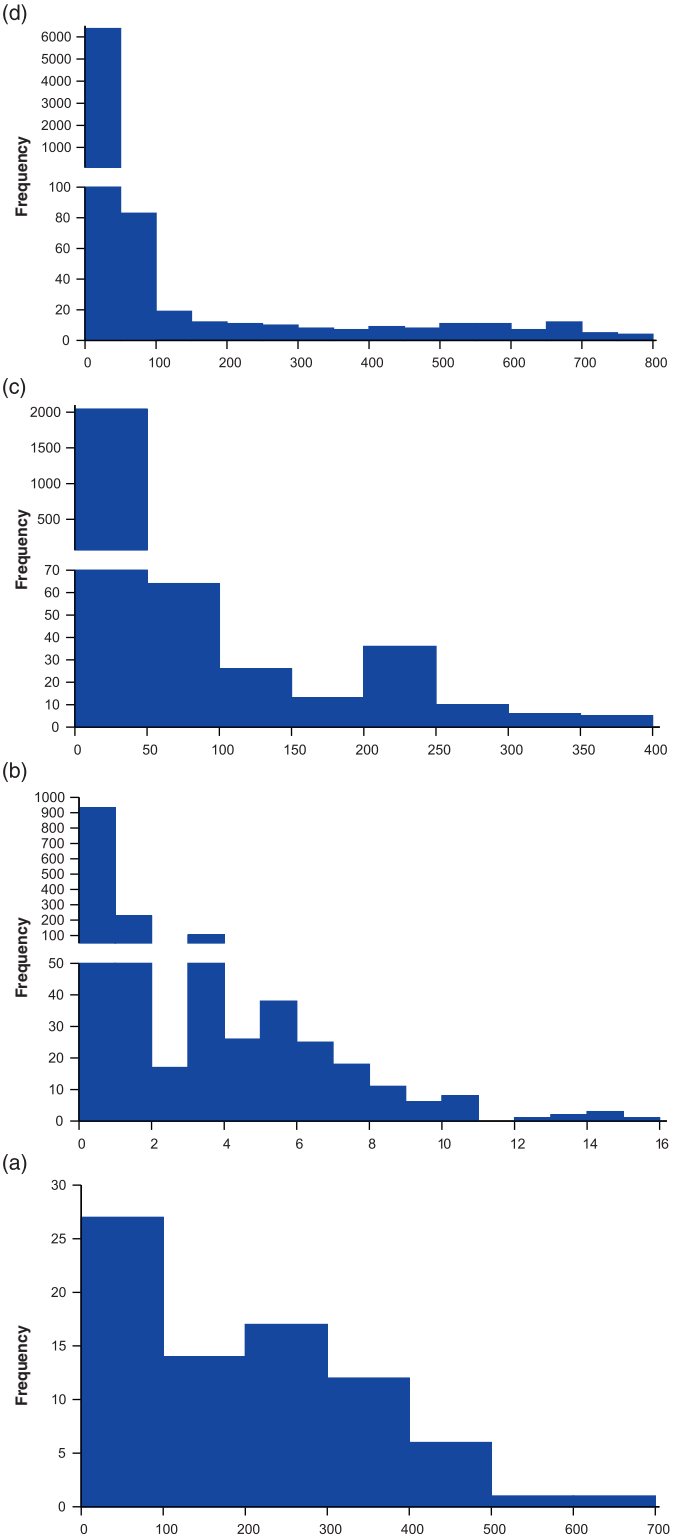


Figure 10. Distribution of Haantjes–Ricci curvature in undirected real networks. (**a**) Karate club, (**b**) Euro road, (**c**) Yeast protein interaction, and (**d**) US Power Grid. Here Haantjes–Ricci curvature is given by Equation (10).

https://doi.org/10.1017/nws.2020.42 Published online by Cambridge University Press

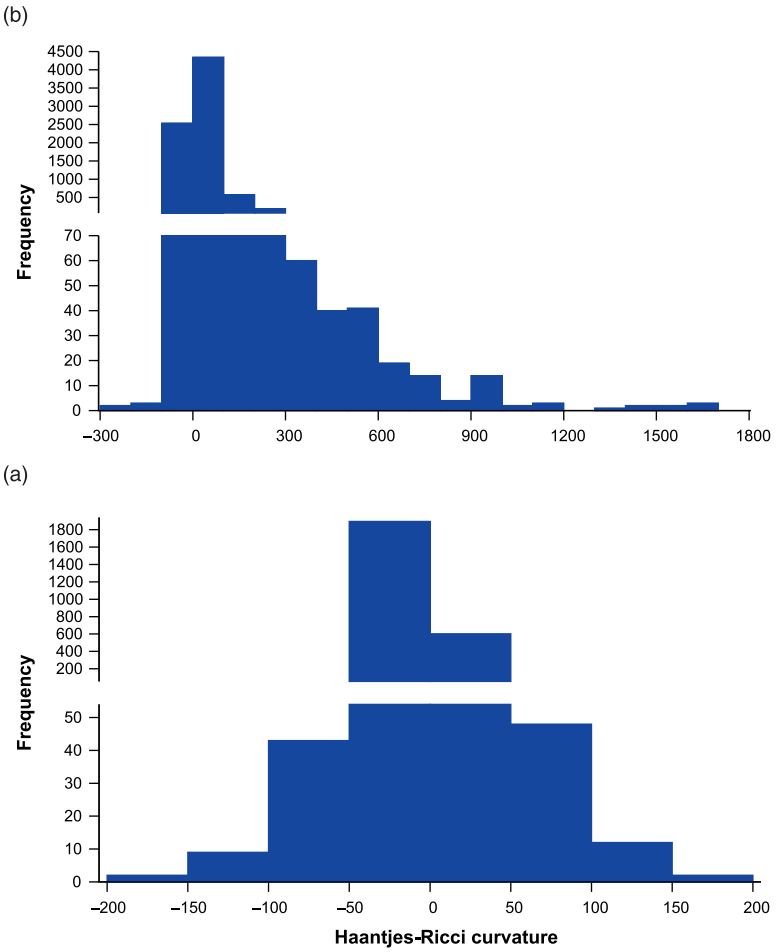


Figure 11. Distribution of Haantjes–Ricci curvature in directed real networks. **(a)** Air traffic control, and **(b)** *E. coli* transcriptional regulatory network. Note that, in this case of directed networks, the Haantjes–Ricci curvature of edges can be negative. Here Haantjes–Ricci curvature is given by Equation (10).

find moderate to high positive correlation between Menger–Ricci and Haantjes–Ricci curvatures even when paths of maximum length up to five are accounted in the computation (Table 2). Thus, one is conduced to the conclusion that the classical ER, WS, and BA models have very little geometric content. This observation is corroborated by the results in Weber et al. (2017) that show that the distribution of Forman–Ricci curvature in real-life networks has little to no resemblance to the one in the models above.

5.4 Comparison of the two metric curvatures with other network measures

We next investigated the correlation of the two notions of metric curvature, Menger–Ricci and Haantjes–Ricci, with other network measures in model and real networks considered here. Specifically, we have studied the correlation with two other notions of Ricci curvature, (augmented) Forman–Ricci curvature and Ollivier–Ricci curvature (Samal et al., 2018; Saucan et al., 2019a), in networks. Specifically, the correlation we computed in the present paper is the classical Pearson correlation coefficient, which takes values in the range $[-1, +1]$. In Table 3, we report

https://doi.org/10.1017/nws.2020.42 Published online by Cambridge University Press

Table 2. Correlation between Menger–Ricci (MR) curvature and Haantjes–Ricci (HR) curvature in model and real networks. Here HR curvature is given by Equation (10)

	MR versus HR curvature computed using paths of maximum length up to			
Network	2	3	4	5
Undirected model networks				
ER with average degree 4	1	0.31	0.14	0.08
ER with average degree 6	1	0.27	0.14	0.09
ER with average degree 8	1	0.24	0.12	0.11
WS with average degree 4	1	0.75	0.55	0.38
WS with average degree 6	1	0.77	0.63	0.44
WS with average degree 8	1	0.82	0.71	0.52
BA with average degree 4	1	0.59	0.52	0.51
BA with average degree 6	1	0.71	0.71	0.71
BA with average degree 8	1	0.88	0.87	0.86
Undirected real networks				
Karate club	1	0.69	0.44	0.27
Euro road	1	0.51	0.37	0.32
Yeast protein interaction	1	0.83	0.74	0.64
US power grid	1	0.82	0.67	0.58
Directed real networks				
Air traffic control	1	0.53	0.39	0.28
E. coli TRN	1	0.83	0.75	0.71

the correlation between augmented Forman–Ricci curvature and Menger–Ricci or Haantjes–Ricci curvature in model and real networks analyzed here. We find no consistent trend in the correlation between augmented Forman–Ricci and Menger–Ricci curvature, or augmented Forman–Ricci and Haantjes–Ricci curvature in model and real networks analyzed here (Table 3). It is seen that there is high negative correlation between augmented Forman–Ricci and Haantjes–Ricci curvature in ER and BA networks, while there is high positive correlation between augmented Forman–Ricci and Menger–Ricci curvature in WS networks (Table 3). In Table 3, we also report the correlation between Ollivier–Ricci curvature and Menger–Ricci or Haantjes–Ricci curvature in model and real networks analyzed here. We again find no consistent trend in the correlation between Ollivier–Ricci and Menger–Ricci curvatures, or Ollivier–Ricci and Haantjes–Ricci curvatures in model and real networks analyzed here (Table 3). Importantly, in recent work (Samal et al., 2018; Saucan et al., 2019a), it was shown that augmented Forman–Ricci and Ollivier–Ricci curvatures have high positive correlation in model and real networks. These observations suggest that the two notions of metric curvature introduced herein capture different aspects of the network organization in comparison to discrete Ricci curvatures previously proposed for geometrical characterization of networks. This fact comes to further accentuate the fundamental observation that it is not possible to find "the best" discrete curvature, but rather the best one suited for a certain task, in a specific type of network. For example, given that Ollivier's curvature has the capability of predicting congestion in communication networks (Wang et al., 2014, 2016), thus it is excellent for the study of such network. However, it may be less suited for social or biological networks, since it is "blind" to cycles of length ≥ 6.

https://doi.org/10.1017/nws.2020.42 Published online by Cambridge University Press

Table 3. Comparison of augmented Forman–Ricci (AFR) curvature and Ollivier–Ricci (OR) curvature with Menger–Ricci (MR) curvature and Haantjes–Ricci (HR) curvature of edges in model and real networks. Here, HR curvature was computed by accounting for paths of maximum length up to 5 in Equation (10)

	AFR curvature versus		OR curvature versus	
Network	MR	HR	MR	HR
Undirected model networks				
ER with average degree 4	0.04	−0.55	0.08	−0.30
ER with average degree 6	0.05	−0.77	0.22	−0.31
ER with average degree 8	0.06	−0.86	0.29	−0.06
WS with average degree 4	0.52	0.02	0.67	0.32
WS with average degree 6	0.65	0.04	0.78	0.46
WS with average degree 8	0.70	0.06	0.80	0.52
BA with average degree 4	−0.37	−0.60	−0.10	−0.36
BA with average degree 6	−0.44	−0.69	0.03	−0.13
BA with average degree 8	−0.56	−0.69	0.17	0.09
Undirected real networks				
Karate club	0.45	−0.22	0.13	−0.42
Euro road	0.02	−0.52	0.02	−0.25
Yeast protein interaction	0.12	−0.04	0.07	−0.10
US power grid	0.11	−0.07	0.16	0.03
Directed real networks				
Air traffic control	0.10	0.13	−0.13	−0.02
E. coli TRN	0.08	0.04	−0.06	−0.07

Finally, we have also studied the correlation between edge betweenness centrality (Freeman, 1977; Girvan & Newman, 2002) and Menger–Ricci or Haantjes–Ricci curvatures in model and real networks (Table 4). We find no consistent trend in the correlation between edge betweenness centrality and Menger–Ricci curvature, or edge betweenness centrality and Haantjes–Ricci curvature in model and real networks analyzed here (Table 4). It is however seen that Menger–Ricci and Haantjes–Ricci curvatures have moderate to high positive correlation with edge betweenness centrality in BA networks (Table 4). We remark that Menger–Ricci curvature, Haantjes–Ricci curvature, (augmented) Forman–Ricci curvature, Ollivier–Ricci curvature, and edge betweenness centrality are edge-centric measures for analysis of networks, and thus, we have compared here these measures in model and real networks.

6. Conclusions and future outlook

In previous work, notions of curvature for networks have been proposed, notably, Ollivier–Ricci curvature (Ollivier, 2009) and Forman–Ricci curvature (Forman, 2003). Ollivier–Ricci curvature is cumbersome to compute in large networks, while Forman–Ricci curvature is much less intuitive. Therefore, in search of simpler and more intuitive notions of curvature for networks and their higher-dimensional generalizations including simplicial and clique complexes, we have adapted here classical metric curvatures of curves, namely, introduced by Menger (1930) and Haantjes (1947), for analysis of complex networks. In particular, we are able to define expressive metric Ricci curvatures for networks, both weighted and unweighted. Moreover, the simple

https://doi.org/10.1017/nws.2020.42 Published online by Cambridge University Press

Table 4. Comparison of edge betweenness centrality with Menger–Ricci (MR) curvature and Haantjes–Ricci (HR) curvature of edges in model and real networks. Here, HR curvature was computed by accounting for paths of maximum length up to 5 in Equation (10)

	Edge betweenness versus	
Network	MR	HR
Undirected model networks		
ER with average degree 4	−0.03	0.35
ER with average degree 6	−0.05	0.51
ER with average degree 8	−0.06	0.56
WS with average degree 4	−0.40	−0.20
WS with average degree 6	−0.56	−0.24
WS with average degree 8	−0.64	−0.27
BA with average degree 4	0.38	0.83
BA with average degree 6	0.52	0.81
BA with average degree 8	0.62	0.76
Undirected real networks		
Karate club	−0.20	0.27
Euro road	−0.02	0.04
Yeast protein interaction	−0.07	0.05
US power grid	−0.03	−0.02
Directed real networks		
Air traffic control	−0.06	−0.13
E. coli TRN	−0.08	−0.06

yet elegant definitions of the metric curvatures introduced here are both computationally efficient (especially, those based on Menger curvature) and extremely versatile (especially, those derived from Haantjes curvature) from the perspective of application to complex networks. In fact, for the analysis of combinatorial (unweighted) polyhedral or simplicial complexes, the definitions of Haantjes–Ricci curvature is shown here to be more expressive than the (augmented) Forman–Ricci curvature as the Haantjes–Ricci curvature accounts for general n-gones and not only triangles like in the case of (augmented) Forman–Ricci curvature.

Previously proposed metric curvature (Saucan, 2012b) based on the *Wald metric curvature* enables easy derivation of convergence results as well as proofs of theoretical results, such as a *PL* version of the classical Bonnet–Myers theorem (Gu & Saucan, 2013). Unfortunately, the metric curvatures proposed in Saucan (2012b) are computationally expensive, and thus, impractical for analysis of large networks. This is in sharp contrast to the simplicity and efficiency of the metric curvatures for networks proposed in the present article.

We have also investigated model and real-world networks using the two notions of metric curvature introduced herein. It is seen that the distribution of Menger–Ricci curvature and Haantjes–Ricci curvature of edges is broader in scale-free BA networks in comparison to random ER networks or small-world WS networks. We also find a positive correlation between Menger–Ricci and Haantjes–Ricci curvature of edges in model and real-world networks; however, this correlation decreases with the increase in the maximum length of paths accounted in Equation (10) for the computation of Haantjes–Ricci curvature. Thereafter, we have compared

https://doi.org/10.1017/nws.2020.42 Published online by Cambridge University Press

the Menger–Ricci or Haantjes–Ricci curvature with augmented Forman–Ricci or Ollivier–Ricci curvature in model and real networks, and no consistent trend in the correlation between Menger–Ricci or Haantjes–Ricci curvature with augmented Forman–Ricci or Ollivier–Ricci curvature was found in analyzed networks. Lastly, we also find no consistent trend in the correlation between edge betweenness centrality and Menger–Ricci or Haantjes–Ricci curvature in analyzed networks. Our empirical results suggest that the metric curvatures introduced herein capture different aspects of the network organization in contrast to previously proposed edge-centric measures, such as Forman–Ricci curvature, Ollivier–Ricci curvature, and edge betweenness centrality, in complex networks. For instance, for combinatorial networks of bounded vertex degree, and in particular for finite networks, large Haantjes–Ricci curvature implies the existence of (arbitrarily) long simple cycles. Thus, the Haantjes–Ricci curvature, even if defined as a local invariant, has the potential of shedding light on the large-scale topological structure of the network.

From a network application perspective, a natural extension is to develop algorithms based on Ricci curvatures introduced herein to detect clusters, modules, or communities in real-world networks, and thereafter, compare the results obtained with algorithms for community detection in networks based on other notions of network curvature (Saucan & Appleboim, 2005; Sia et al., 2019; Ni et al., 2019). Another application that imposes itself in view of the geodesic curvature role that Haantjes (and Menger) curvature plays in a vast, highly relevant class of metric spaces (see Appendix), is to use metric curvature for routing and hole detection ends. Furthermore, another interesting exploration would be to investigate the correlation between the metric notions of curvature introduced herein and hyperbolic embeddings of networks. In particular, it is worthwhile to investigate the extent to which the curvatures can predict the values obtained using the inferred hyperbolic distances among vertices in embeddings considered in previous work (Boguná et al., 2010) and also study the extent to which these values are in concordance with the curvatures measured on the given network. Among the theoretical problems naturally arising from this work, one would like to first and foremost prove such results as a fitting analogue of the fundamental global Gauss–Bonnet theorem (which has important consequences in the study of long time evolution of networks (Weber et al., 2018)), as well as a fitting Bonnet–Myers theorem. Another important direction of theoretical study, that also has clear implications in real-life, large-scale applications, is to determine the full extent of the local-to-global properties of the new invariants introduced in the present manuscript.

Acknowledgments. The authors would like to thank the anonymous reviewers for their comments which have helped improve the manuscript.

Funding. JJ and ES were partly supported by the German-Israeli Foundation Grant I-1514-304.6/2019. AS would like to thank Max Planck Society, Germany, for the award of a Max Planck Partner Group in Mathematical Biology.

Conflicts of interest. None.

Notes

1 Note that the field assigned to the hexagonal tilling for Ollivier–Ricci curvature in Table 1 is marked as "–", since in this case the Ollivier–Ricci curvature is not applicable, see (Cushing & Kamtue, 2019). Also, in Table 1, $\mathrm{Ric}_H(e)$ denotes the strong Haantjes–Ricci curvature given by Equation (18).

2 We suggest the name *strong local metrics* for those sets of positive weights that satisfy the generalized triangle inequality $w(v_0, v_1, \ldots, v_n, v_{n+1}) < w(v_0, v_n)$, for any elementary 1-cycle $v_0, v_1, \ldots, v_n, v_0$.

References

Albert, R., & Barabási, A. L. (2002). Statistical mechanics of complex networks. *Reviews of Modern Physics*, *74*(1), 47.

Asoodeh, S., Gao, T., & Evans, J. (2018). Curvature of hypergraphs via multi-marginal optimal transport. In *2018 IEEE Conference on Decision and Control (CDC)* (pp. 1180–1185). IEEE.

https://doi.org/10.1017/nws.2020.42 Published online by Cambridge University Press

Barabási, A. L., & Albert, R. (1999). Emergence of scaling in random networks. *Science*, *286*(5439), 509–512.
Bianconi, G., & Rahmede, C. (2017). Emergent hyperbolic network geometry. *Scientific Reports*, *7*, 41974.
Blumenthal, L. M. (1953) *Distance Geometry – Theory and Applications*. Claredon Press.
Blumenthal, L. M. & Menger, K. (1970) *Studies in geometry*. Freeman and Co.
Boguná, M., Papadopoulos, F., & Krioukov, D. (2010). Sustaining the internet with hyperbolic mapping. *Nature Communications*, *1*(1), 1–8.
Boguná, M., Bonamassa, I., De Domenico, M., Havlin, S., Krioukov, D., & Serrano, M. (2020). Network geometry. *arXiv preprint arXiv:2001.03241*.
Burago, D., Burago, Y., & Ivanov, S. A. (2001). *A course in metric geometry*. Graduate Studies in Mathematics, vol. 33. Providence, RI: American Mathematical Society.
Cushing, D., & Kamtue, S. (2019). Long-scale Ollivier Ricci curvature of graphs. *Analysis and Geometry in Metric Spaces*, *7*(1), 22–44.
Dodziuk, J., & Kendall, W. S. (1986). Combinatorial Laplacians and Isoperimetric inequality. In K. D. Elworthy (Ed.), *From local times to global geometry, control and physics*. Pitman Research Notes in Mathematics Series, vol. 150 (pp. 68–74). London, UK: Prentice Hall Press.
Dorogovtsev, S. N., & Mendes, J. F. F. (2013). *Evolution of networks: From biological nets to the Internet and WWW*. Oxford University Press.
Eckmann, J., & Moses, E. (2002). Curvature of co-links uncovers hidden thematic layers in the world wide web. *Proceedings of the National Academy of Sciences USA*, *99*(9), 5825–5829.
Epstein, D. B. A., Paterson, M. S., Cannon, J. W., Holt, D. F., Levy, S. V., & Thurston, W. P. (1992). *Word Processing in Groups*. USA: A. K. Peters Ltd.
Erdös, P., & Rényi, A. (1961). On the evolution of random graphs. *Bull. Inst. Internat. Statist.*, *38*(4), 343–347.
Farooq, H., Chen, Y., Georgiou, T. T., Tannenbaum, A., & Lenglet, C. (2019). Network curvature as a hallmark of brain structural connectivity. *Nature Communications*, *10*(1), 1–11.
Forman, R. (2003). Bochner's method for cell complexes and combinatorial Ricci curvature. *Discrete and Computational Geometry*, *29*(3), 323–374.
Freeman, L. C. (1977). A set of measures of centrality based on betweenness. *Sociometry*, *40*, 35–41.
Girvan, M., & Newman, M.E.J. (2002). Community structure in social and biological networks. *Proceedings of the National Academy of Sciences USA*, *99*(12), 7821–7826.
Gromov, M. (2007). *Metric structures for Riemannian and non-Riemannian spaces*. Birkhäuser Boston.
Gu, D. X., & Saucan, E. (2013). Metric Ricci curvature for PL manifolds. *Geometry*, *2013*, 12. doi: 10.1155/2013/694169
Haantjes, J. (1947). Distance geometry. Curvature in abstract metric spaces. *Proc. Kon. Ned. Akad. v. Wetenseh., Amsterdam*, *50*, 302–314.
Horak, D., & Jost, J. (2013). Spectra of combinatorial Laplace operators on simplicial complexes. *Advances in Mathematics*, *244*, 303–336.
Janson, S. (2015). *Lecture notes on Euclidean, spherical and hyperbolic trigonometry*.
Jeong, H., Mason, S. P., Barabási, A. L., & Oltvai, Z. N. (2001). Lethality and centrality in protein networks. *Nature*, *411*(6833), 41–42.
Jost, J. (2017). *Riemannian geometry and geometric analysis* (7th ed.). Berlin: Springer International Publishing.
Kay, D. C. (1980). Arc curvature in metric spaces. *Geometriae Dedicata*, *9*(1), 91–105.
Keller, M. (2015). Intrinsic metrics on graphs: A survey. In D. Mugnolo (ed.), *Mathematical technology of networks* (pp. 81–119). Cham: Springer International Publishing.
Krioukov, D., Papadopoulos, F., Kitsak, M., Vahdat, A., & Boguná, M. (2010). Hyperbolic geometry of complex networks. *Physical Review E*, *82*(3), 036106.
Kunegis, J. (2013). Konect: the Koblenz network collection. In *Proceedings of the* 22^{nd} *international conference on world wide web companion* (pp. 1343–1350). New York, NY, USA: ACM.
Leskovec, J., Kleinberg, J., & Faloutsos, C. (2007). Graph evolution: Densification and shrinking diameters. *ACM Transactions on Knowledge Discovery from Data (TKDD)*, *1*(1), 2.
Menger, K. (1930). Untersuchungen über allgemeine Metrik. Vierte Untersuchung. Zur Metrik der Kurven. *Mathematische Annalen*, *103*, 466–501.
Milo, R., Shen-Orr, S., Itzkovitz, S., Kashtan, N., Chklovskii, D., & Alon, U. (2002). Network motifs: simple building blocks of complex networks. *Science*, *298*(5594), 824–827.
Newman, M. E. J. (2010). *Networks: An introduction*. Oxford, UK: Oxford University Press.
Ni, C., Lin, Y., Gao, J., Gu, X. D., & Saucan, E. (2015). Ricci curvature of the Internet topology. In *2015 IEEE conference on computer communications (INFOCOM)* (pp. 2758–2766). Hong Kong: IEEE.
Ni, C., Lin, Y., Luo, F., & Gao, J. (2019). Community detection on networks with Ricci flow. *Scientific Reports*, *9*(1), 1–12.
Ollivier, Y. (2009). Ricci curvature of Markov chains on metric spaces. *Journal of Functional Analysis*, *256*(3), 810–864.
Pauc, C. (1936). Courbure dans les espaces métriques. *Atti Acad. di Lincei, Serie 6*, *24*, 109–115.
Perelman, G. (1991). Alexandrov's spaces with curvature bounded from below II. *preprint*.
Plaut, C. (2002). *Metric spaces of curvature* $\geq k$. *Handbook of geometric topology* (pp. 819–898). Elsevier, Amsterdam.

https://doi.org/10.1017/nws.2020.42 Published online by Cambridge University Press

Salgado, H., Peralta-Gil, M., Gama-Castro, S., Santos-Zavaleta, A., Muniz-Rascado, L., Garcia-Sotelo, J. S., . . . Collado-Vides, J. (2013). RegulonDB v8.0: Omics data sets, evolutionary conservation, regulatory phrases, cross- validated gold standards and more. *Nucleic Acids Research*, *41*(D1), D203–D213.

Samal, A., Sreejith, R. P., Gu, J., Liu, S., Saucan, E., & Jost, J. (2018). Comparative analysis of two discretizations of Ricci curvature for complex networks. *Scientific Reports*, *8*, 8650.

Sandhu, R., Georgiou, T., Reznik, E., Zhu, L., Kolesov, I., Senbabaoglu, Y., & Tannenbaum, A. (2015). Graph curvature for differentiating cancer networks. *Scientific Reports*, *5*, 12323.

Saucan, E. (2012a). Isometric embeddings in imaging and vision: Facts and fiction. *Journal of Mathematical Imaging and Vision*, *43*(2), 143–155.

Saucan, E. (2012b). On a construction of Burago and Zalgaller. *Asian Journal of Mathematics*, *16*(4), 587–606.

Saucan, E. (2016). Metric curvatures and their applications I. *Geometry, Imaging and Computing*, *2*(4), 257–334.

Saucan, E., & Appleboim, E. (2005). Curvature based clustering for dna microarray data analysis. In *Iberian conference on pattern recognition and image analysis* (pp. 405–412). Berlin, Heidelberg: Springer.

Saucan, E., & Weber, M. (2018). Forman's Ricci curvature-from networks to hypernetworks. In *International conference on complex networks and their applications* (pp. 706–717). Cham: Springer.

Saucan, E., Sreejith, R. P., Vivek-Ananth, R. P., Jost, J., & Samal, A. (2019a). Discrete Ricci curvatures for directed networks. *Chaos, Solitons & Fractals*, *118*, 347–360.

Saucan, E., Samal, A., & Jost, J. (2019b). A simple differential geometry for networks and its generalizations. In *International conference on complex networks and their applications* (pp. 943–954). Cham: Springer.

Sia, J., Jonckheere, E., & Bogdan, P. (2019). Ollivier-Ricci curvature-based method to community detection in complex networks. *Scientific Reports*, *9*(1), 1–12.

Sreejith, R. P., Mohanraj, K., Jost, J., Saucan, E., & Samal, A. (2016). Forman curvature for complex networks. *Journal of Statistical Mechanics: Theory and Experiment*, *063206*.

Stone, D. A. (1973). Sectional curvatures in piecewise linear manifolds. *Bull. Amer. Math. Soc.*, *79*, 1060–1063.

Stone, D. A. (1976). A combinatorial analogue of a theorem of Myers. *Illinois Journal of Mathematics*, *20*(1), 12–21.

Šubelj, L., & Bajec, M. (2011). Robust network community detection using balanced propagation. *The European Physical Journal B*, *81*(3), 353–362.

Sundaresan, S.R., Fischhoff, I.R., Dushoff, J., & Rubenstein, D.I., (2007). Network metrics reveal differences in social organization between two fission-fusion species, Grevy's zebra and onager. *Oecologia*, *151*(1), 140–149.

Thurston, W. P. (1997). *Three-dimensional geometry and topology*. Princeton, NJ: Princeton University Press.

Vaserstein, L. N. (1969). Markov processes over denumerable products of spaces, describing large systems of automata. *Problemy Peredachi Informatsii*, *5*(3), 64–72.

Villani, C. (2009). *Optimal transport: old and new*. Grundlehren der mathematischen Wissenschaften, vol. 338. Berlin Heidelberg: Springer-Verlag.

Wang, C., Jonckheere, E., & R. Banirazi, R. (2014) Wireless network capacity versus Ollivier-Ricci curvature under Heat Diffusion (HD) protocol. In *2014 American control conference (ACC)* (pp. 3536–3541). Portland, OR: IEEE.

Wang, C., Jonckheere, E., & R. Banirazi, R. (2014) Interference constrained network performance control based on curvature control. In *2016 American control conference (ACC)* (pp. 6036–6041). Boston, MA: IEEE.

Watts, D. J., & Strogatz, S. H. (1998). Collective dynamics of small-world networks. *Nature*, *393*(6684), 440–442.

Weber, M., Saucan, E., & Jost, J. (2017). Characterizing complex networks with Forman-Ricci curvature and associated geometric flows. *Journal of Complex Networks*, *5*(4), 527–550.

Weber, M., Saucan, E., & Jost, J. (2018). Coarse geometry of evolving networks. *Journal of complex networks*, *6*(5), 706–732.

Zachary, W. W. (1977). An information flow model for conflict and fission in small groups. *Journal of Anthropological Research*, *33*(4), 452–473.

Zeng, W., Sarkar, R., Luo, F., Gu, X. D., & Gao, J. (2010). Resilient routing for sensor networks using hyperbolic embedding of universal covering space. In *2010 IEEE conference on computer communications (INFOCOM)* (pp. 1–9). San Diego, CA: IEEE.

Appendix A. Metric curvatures and classical curvature of curves

Both Menger curvature (Menger, 1930) and Haantjes curvature (Haantjes, 1947) were devised as generalizations to metric spaces of the classical notion of curvature for smooth plane curves. Therefore, it is only natural to ask whether they represent good approximations of the classical invariant. Indeed, as expected, this turns out to be the case for both metric curvatures. To state these results more formally, we need the following definition:

Definition A.1. Let (M, d) be a metric space and let $p \in M$ be an accumulation point. We say that M has *Menger curvature* $\kappa_M(p)$ at p iff for any $\varepsilon > 0$, there exists $\delta > 0$, such that for any triple of points p_1, p_2, p_3, satisfying $d(p, p_i) < \delta,\ i = 1, 2, 3$, the following inequality holds: $|K_M(p_1, p_2, p_3) - \kappa_M(p)| < \varepsilon$.

https://doi.org/10.1017/nws.2020.42 Published online by Cambridge University Press

While the corresponding definition for Haantjes curvature was essentially introduced in Equation (7), we again state the same more formally here:

Definition A.2. Let (M, d) be a metric space and let $c{:}I = [0,1] \xrightarrow{\sim} M$ be a homeomorphism, and let $p, q, r \in c(I),\ q, r \neq p$. Denote by $\widehat{qr}$ the arc of $c(I)$ between q and r, and by qr line segment from q to r. We say that the curve $c = c(I)$ has *Haantjes* (or *Finsler-Haantjes*) *curvature* $\kappa_H(p)$ at the point p iff:

$$\kappa_H^2(p) = 24 \lim_{q,r \to p} \frac{l(\widehat{qr}) - d(q,r)}{\left(l(\widehat{qr})\right)^3} \ , \tag{28}$$

where $l(\widehat{qr})$ denotes the length, in the intrinsic metric induced by d, of $\widehat{qr}$. Note that the above definition is not the precise one used in this work.

For points or arcs where Haantjes curvature exists, we have $\frac{l(\widehat{qr})}{d(q,r)} \to 1$ as $d(q,r) \to 0$ (see Haantjes (1947)), and therefore, κ_H can be defined by (see, e.g. Kay (1980))

$$\kappa_H^2(p) = 24 \lim_{q,r \to p} \frac{l(\widehat{qr}) - d(q,r)}{\left(d(q,r)\right)^3} \ . \tag{29}$$

In the setting of graphs or networks, we prefer the above alternative form of the definition of Haantjes curvature which is even more intuitive and simpler to use.

As expected, Haantjes curvature for smooth curves in the Euclidean plane (or space) coincides with the standard (differential) notion. More precisely, we have the following result, see Haantjes (1947).

Theorem A.3. *Let $c \in \mathscr{C}^3$ be smooth curve in $\mathbb{R}^3$ and let $p \in c$ be a regular point. Then the metric curvature $\kappa_H(p)$ exists and equals the classical curvature of γ at p.*

A similar result also holds for Menger curvature. However, we will arrive at the result in an indirect fashion which will enable us to establish the connection between the two types of metric curvature used here. First, note that although the Haantjes curvature exhibits additional flexibility in the network context in comparison to the Menger curvature, the formal definition of Haantjes curvature in the setting of metric spaces is a more restricted notion than the Menger curvature, since it can be employed only for rectifiable curves. However, the following theorem due to Pauc (1936) holds:

Theorem A.4. *Let (X, d) be a metric continuum, and consider $p \in X$. If $\kappa_M(p)$ exists, then X is a rectifiable arc in a neighborhood of p.*

Corollary A.5. *Let (X, d) be a metric arc. If $\kappa_M(p)$ exists at all points $p \in X$, then X is rectifiable.*

In consequence, the existence of one of the considered metric curvatures implies the existence of the other. In fact, the two definitions coincide whenever they both are applicable:

Theorem A.6. *(Haantjes, 1947) Let c be a rectifiable arc in a metric space (M, d), and let $p \in c$. If κ_M and κ_H exist, then they are equal.*

Furthermore, it turns out that another important property of classical curvature, namely characterization of geodesics via *geodesic curvature* (see, e.g. Jost (2017)) is also captured, at least for a large class of metric spaces, by Haantjes curvature (hence, due to Theorem A.6 above, by Menger's curvature as well). More precisely, we have the following result:

Theorem A.7. *(Haantjes, 1947) Let (X, d) be a metric space and let $\gamma \subset X$ be a* Ptolemaic *arc (in the induced metric). γ is a geodesic segment if $\kappa_H(p) = 0$, for any $p \in \gamma$.*

While we do not bring here the technical definition of Ptolemaic metric spaces, since this would expand the present text in an inordinate manner and we only refer the reader to Blumenthal (1953) and Blumenthal & Menger (1970). We wish to underline that Euclidean and Hyperbolic spaces are Ptolemaic, thus one can apply the theorem above to networks embedded in such spaces.

Cite this article: Saucan E., Samal A. and Jost J. (2021). A simple differential geometry for complex networks. *Network Science* **9**, S106–S133. https://doi.org/10.1017/nws.2020.42

https://doi.org/10.1017/nws.2020.42 Published online by Cambridge University Press